

STUDY OF HEAVY QUARKONIA SPECTRA IN THE QUARK MODEL

A THESIS SUBMITTED TO
THE GRADUATE SCHOOL OF NATURAL AND APPLIED SCIENCES
OF
MIDDLE EAST TECHNICAL UNIVERSITY

BY

TAYLAN TAKAN

IN PARTIAL FULFILLMENT OF THE REQUIREMENTS
FOR
THE DEGREE OF MASTER OF SCIENCE
IN
PHYSICS

FEBRUARY 2012

Approval of the thesis:

STUDY OF HEAVY QUARKONIA SPECTRA IN THE QUARK MODEL

submitted by **TAYLAN TAKAN** in partial fulfillment of the requirements for the degree of **Master of Science in Physics Department, Middle East Technical University** by,

Prof. Dr. Canan Özgen
Dean, Graduate School of **Natural and Applied Sciences**

Prof. Dr. Mehmet T. Zeyrek
Head of Department, **Physics**

Prof. Dr. Altuğ Özpıneci
Supervisor, **Physics Department, METU**

Examining Committee Members:

Prof. Dr. Valeri ZAMIRALOV
Moscow State University, Institute of Nuclear Physics

Prof. Dr. Altuğ Özpıneci
Middle East Technical University, Department of Physics

Prof. Dr. Mehmet ZEYREK
Middle East Technical University, Department of Physics

Prof. Dr. Takhmasib ALIEV
Middle East Technical University, Department of Physics

Assoc. Prof. Dr. İsmail TURAN
Middle East Technical University, Department of Physics

Date:

I hereby declare that all information in this document has been obtained and presented in accordance with academic rules and ethical conduct. I also declare that, as required by these rules and conduct, I have fully cited and referenced all material and results that are not original to this work.

Name, Last Name: TAYLAN TAKAN

Signature :

ABSTRACT

STUDY OF HEAVY QUARKONIA SPECTRA IN THE QUARK MODEL

Takan, Taylan

M.Sc., Department of Physics

Supervisor : Prof. Dr. Altuğ Özpineci

February 2012, 51 pages

Conventional Heavy Quarkonium systems, Charmonium and Bottomonium, are believed to be composed of a heavy quark and anti-quark pair. These systems are investigated by different methods resulting from different approaches to Quantum Chromodynamics (QCD), such as Lattice QCD, Effective Theories and Sum Rules. In this thesis we study the spectrum of Charmonium and Bottomonium using a non-relativistic Quark Model. Assuming one gluon exchange for the short distances and a linear confining potential for long distances we derive Breit-Fermi interaction Hamiltonian and calculate the spectra arising from this Hamiltonian. Also we calculate the partial widths of E1 and M1 radiative decays.

Keywords: QCD, Quark Model, Charmonium, Bottomonium, Heavy Quarkonia

ÖZ

AĞIR KUARKONYA TAYFLARININ KUARK MODELİ İLE İNCELENMESİ

Takan, Taylan

Yüksek Lisans, Fizik Bölümü

Tez Yöneticisi : Prof. Dr. Altuğ Özpıneci

Şubat 2012, 51 sayfa

Çarmonyum ve Botomonyum gibi olağan ağır kuarkonyum sistemleri ağır kuark anti-kuark çiftlerinden oluşurlar. Bu sistemler KRD'ye yapılan farklı yaklaşımlarla (Kafes KRD, Efektif Alan Teorileri ve Toplam Kuralları gibi) elde edilen çeşitli metodlarla incelenmektedir. Bu tezde Çarmonyum ve Botomonyum tayfları rölativistik olmayan Kuark Modeli ile incelenmektedir. Kısa mesafelerde tek gluon değişimi, uzun mesafelerde doğrusal kafesleyici potansiyel varsayılarak, Breit-Fermi etkileşim Hamiltonu çıkarılmıştır ve bu Hamiltonun yarattığı tayflar hesaplanmıştır. Ayrıca E1 ve M1 ışınımsal bozunumları hesaplanmıştır.

Anahtar Kelimeler: KRD, Kuark Modeli, Çarmonyum, Botomonyum, Ağır Kuarkonyum

In loving memory of Ali Takan

ACKNOWLEDGMENTS

I would like to express my deepest gratitude to my advisor, Prof. Dr. Altuđ Özpineci not only for his support and guidance but also for motivating and helping me with his insight.

I am grateful to Prof. Dr. Mehmet T. Zeyrek for his constant guidance throughout my undergraduate and graduate years. Without his generous support, especially during the most challenging times, this thesis would not be possible.

I would like to thank fellow students, Nader Ghazanfari, Kamil ınar, Baha Dinel, Muhammed Mira Serim, Sinan Deđer, Ozan Yılırım, Seluk Bilmiř, Utku Can, Ulař Özdem, Vedat Tanrıverdi, Didem ebi, Mehmet Ali Olpak and Deniz Deveciođlu for their company.

I would like to thank Ceren Sibel Sayın for patiently being with me throughout very hard years and devoting her support during the writing of this thesis.

I owe many thanks to my parents, Zuhul and Muslihittin Takan for their encouragement, support and understanding.

TABLE OF CONTENTS

ABSTRACT	iv
ÖZ	v
ACKNOWLEDGMENTS	vii
TABLE OF CONTENTS	viii
LIST OF TABLES	x
LIST OF FIGURES	xi
CHAPTERS	
1 INTRODUCTION	1
2 QUARK MODEL	4
2.1 One-Gluon Exchange	5
2.2 Breit Interaction	6
2.3 Potential Model	11
2.3.1 The Cornell Potential	11
2.3.2 Breit-Fermi Interactions	12
2.3.2.1 Increase of Relativistic Mass	13
2.3.2.2 Retardation of Potential	13
2.3.2.3 Darwin Term	14
2.3.2.4 Spin-Spin Interaction	15
2.3.2.5 Spin-Orbit Coupling	15
2.3.2.6 Tensor Force	16
3 METHOD	17
3.1 Schrödinger Equation with Central Potential	17
3.1.1 Simple Harmonic Oscillator in Three Dimensions	18
3.1.2 Method	19

4	SPECTRUM AND RADIATIVE TRANSITIONS	22
4.1	Charmonium	22
4.2	Bottomonium	23
4.3	E1 and M1 Radiative Transitions	26
5	CONCLUSION	38
	REFERENCES	40
	APPENDICES	
A	FOLDY-WOUTHUYSEN TRANSFORMATION	43
B	TENSOR INTERACTION COEFFICIENTS	48

LIST OF TABLES

TABLES

Table 4.1	Calculated and experimental values, [28], of $c\bar{c}$ and $b\bar{b}$ spectra. The dagger shows which states are used for the fit	25
Table 4.2	Partial widths of, $c\bar{c}$ E1 radiative transitions from S states.	30
Table 4.3	Partial widths of, $b\bar{b}$ E1 radiative transitions from S states.	31
Table 4.4	Partial widths of, $c\bar{c}$ E1 radiative transitions from P states.	32
Table 4.5	Partial widths of, $c\bar{c}$ E1 radiative transitions from P states (continued).	33
Table 4.6	Partial widths of, $b\bar{b}$ E1 radiative transitions from P states.	34
Table 4.7	Partial widths of, $b\bar{b}$ E1 radiative transitions from P states (continued).	35
Table 4.8	Partial widths of, $c\bar{c}$ M1 radiative transitions.	36
Table 4.9	Partial widths of, $b\bar{b}$ M1 radiative transitions.	37

LIST OF FIGURES

FIGURES

Figure 2.1 Feynman Diagram for s-channel	5
Figure 2.2 Feynman Diagram for t-channel	5
Figure 4.1 Charmonium Spectrum Showing Experimental Measurements(Black) vs. Fitted Mass Values (Blue, dotted).	23
Figure 4.2 Squared radial wavefunctions for η_c (blue straight) and J/ψ (red dashed) .	24
Figure 4.3 Squared radial wavefunctions for $\eta_c(2S)$ (blue straight) and $J/\psi(2S)$ (red dashed).	24
Figure 4.4 Squared radial wavefunctions for χ_0 (blue straight), χ_1 (red dashed), h_c (green dot-dashed) and χ_2 (black-thick)	26
Figure 4.5 Bottomonium Spectrum Showing Experimental Measurements(Black) vs. Fitted Mass Values (Blue, dotted).	27
Figure 4.6 Squared reduced radial wavefunctions for η_b (blue straight) and $\Upsilon(1S)$ (red dashed)	27
Figure 4.7 Squared radial wavefunctions for $\eta_b(2S)$ (blue straight) and $\Upsilon(2S)$ (red dashed)	28
Figure 4.8 Squared radial wavefunctions for χ_{b0} (blue straight), χ_{b1} (red dashed), h_b (green dot-dashed) and χ_{b2} (black-thick)	28
Figure 4.9 Squared radial wavefunctions for $Y(1D)$	29

CHAPTER 1

INTRODUCTION

Quarks together with leptons constitute the ordinary matter content of our universe. Physics of quarks and the force carriers between them, gluons, is governed by Quantum Chromodynamics (QCD). Unlike Quantum Electrodynamics or the unified Electroweak theory, Quantum Chromodynamics does not readily supply us with physical observables such as the mass of the bound states of quarks and anti-quarks called hadrons nor the transitions between these different states.

This challenge presented by QCD can be attributed to the several features that are not present in other local gauge field theories. One of these characteristic properties is the non-Abelian nature of theory, resulting from the fact that the force carriers carry color charge themselves. Therefore in QCD one must consider interactions between the gauge bosons in addition to the interaction between fermions and the gauge bosons.

Apart from the non-Abelian nature one must also embark upon three important phenomena that QCD presents, namely, asymptotic freedom, confinement and dynamical breaking of chiral symmetry.

Asymptotic freedom of QCD dictates that the coupling constant, α_s , depends on the momentum transfer in a process. For soft processes, which include low momentum exchange, α_s is large, therefore perturbation theory can not be used. α_s becomes small only at large momentum values. These processes are called hard processes. In terms of the momentum exchange, Q^2 , the lowest order QCD corrections to α_s can be parameterized as,

$$\alpha_s(Q^2) = \frac{12\pi}{(33 - 2n_f) \ln(Q^2/\Lambda^2)} \quad (1.1)$$

where n_f is the number of fermion flavors with mass below Q , and $\Lambda \approx \Lambda_{\text{QCD}}$ is the charac-

teristic scale of QCD measured as $\approx 200\text{MeV}$ [28]. Although it seems at first sight that hard processes can be calculated perturbatively, it is generally not the case and one needs further relation between partons and the observed hadrons and these relations, called structure and fragmentation functions, can not be calculated perturbatively. As an example; the decay of $c\bar{c}$ into gluons can be calculated perturbatively, however to calculate the annihilation of J/Ψ into light hadrons one needs the wave function of the $c\bar{c}$ system at the origin, $\Psi(0)$, which is not calculable by the perturbation theory [32].

As mentioned above, for the low momentum exchange, or in other words for the long distances, the perturbation theory fails completely and we face a new phenomenon; confinement. Flux tube model gives a qualitative explanation of confinement. According to this model as the distance between quark and an anti-quark, or two quarks, increases the field lines bunch up to form a flux tube, resulting in a potential energy that depends approximately linearly on the distance,

$$\sim \sigma r \tag{1.2}$$

characterized by the string constant, σ . If the distance, therefore energy is increased further a new quark-anti-quark pair forms resulting in total two colorless hadrons. Although as of now there is no satisfactory explanation of the confinement which is based solely on the QCD Lagrangian, there are several approaches that hints confinement. The lattice models are successful in simulating this phenomena and calculating the string tension [7]. On the theoretical side there is work in progress, which suggests that QCD potential may be expressed as Coulomb plus a linear potential [41].

The third important concept of QCD is the dynamical breaking of chiral symmetry. Symmetry breaking can be explained qualitatively by considering the QCD Lagrangian for N quark flavors with massless quarks,

$$L = i\Sigma_i \bar{q} \left[\partial_\mu - ig_s \Sigma_a \frac{1}{2} \lambda^a A_\mu^a \right] \gamma^\mu q_i - \frac{1}{4} \Sigma_a F_{\mu\nu}^a F^{\mu\nu a} \tag{1.3}$$

where the mass term, $-\Sigma_i \bar{q} m_i q_i$, is dropped. In such a theory there is an exact chiral $SU(N) \times SU(N)$ symmetry but this symmetry breaks down to $SU(N)$ because of the non-vanishing expectation value of the QCD vacuum. The Goldstone bosons corresponding to this symmetry breaking are the pseudoscalar mesons.

To deal with the mentioned aspects of the QCD, different methods are available such as QCD sum rules, Effective Theories, Lattice QCD and AdS/QCD correspondence.

This thesis is concerned with the Quark Model approach. Compared with the other methods mentioned above Quark Model may seem inadequate as it lacks the rigor present in other models as Quark Model is based mostly on intuition and include bold assumptions. The answer to these concerns is that Quark Model works in it's own domain, as proved by numerous studies [23].

Today with the experiments providing us greater precision on the spectrum and decay widths [45] more than ever and the discovery of the unconventional Ψ and Υ bound states [2][12], which can not be explained with the usual $q\bar{q}$ picture, the intuitive nature of Quark Model may leverage it's use as a testing ground for new ideas.

The purpose of this thesis is to investigate the basic assumptions and intuitive picture behind the Quark Model. To serve this purpose we think that the Charmonium and Bottomonium spectra provides us an unique opportunity; we believe the study of low lying states that have been the subject of may fruitful analysis [18][17][19][43][27][36] can enable us to investigate the basic assumptions and newly found higher mass states and unconventional states [6][42] which are believed to fall outside the assumptions of the Quark Model may help draw the boundaries of the quark model or even expand them.

CHAPTER 2

QUARK MODEL

The physics of hadrons is multi-dimensional. When considering the spectroscopy we face increasing values of radius at excited state, which is dominated by non-perturbative effects, but when considering decays we deal with hard processes occurring at short distances which in part allows perturbative approach. Therefore the challenge before the Quark model is to describe a system with two different regimes. To accomplish this hard task the Quark Model, in its simplest form assumes that the interactions of quarks to be a two-body potential and quarks to be heavy enough that they satisfy the non-relativistic Schrodinger equation. In doing so it disregards the gluonic degrees of freedom in the QCD Lagrangian [32].

In the perturbative regime, the potential arising from QCD is simply Coulomblike, this follows from the fact that for small α_s we only need to consider one gluon exchange, as it will be the dominant process. One gluon exchange between a quark and an anti-quark have the same form as electron-anti-electron scattering which has the form of Coulomb interaction. This similarity between quarkonia and positronium allows heavy quarkonium physics to be a testing ground for QCD.

However this similarity holds only for short distances, and we are still left with the delicate question about of the form and the origin of the confining potential. In the early days of the Quark Model much debate has been made on the form of the confining potential [37]. Today we are closer more than ever to a complete description of the confinement and the form of the confining potential. The quantitative picture is provided mainly by the Lattice QCD calculations which predict a linear potential with the string tension around 0.15 GeV^2 [30]. Other approaches confirm the form, if not the value the potential obtained from lattice simulations.

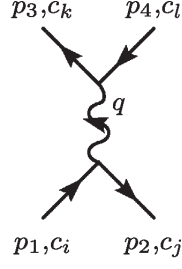


Figure 2.1: Feynman Diagram for s-channel

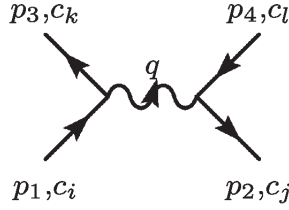


Figure 2.2: Feynman Diagram for t-channel

2.1 One-Gluon Exchange

To motivate the coulomb potential we begin by considering scattering of a quark from anti-quark. For the s-channel, using Feynman rules, we obtain,

$$-i\mathcal{M} = [\bar{u}(3)c_{3k}^\dagger] \left(-i\frac{\alpha_s}{2} \lambda_{kl}^\alpha \gamma^\mu \right) [c_{4l}v(4)] \left(-i\frac{g_{\mu\nu\delta\alpha\beta}}{q^2} \right) [\bar{v}(2)c_{2j}^\dagger] \left(-i\frac{\alpha_s}{2} \lambda_{ji}^\beta \gamma^\nu \right) [c_{1i}u(1)] \quad (2.1)$$

Therefore the s-channel amplitude is given by,

$$\mathcal{M} = \left(\frac{1}{4} c_{3k}^\dagger c_{4l} c_{2j}^\dagger c_{1i} \lambda_{kl}^\alpha \lambda_{ji}^\alpha \right) \left(-\frac{\alpha_s^2}{q^2} \right) [\bar{u}(3)\gamma^\mu u(1)] [\bar{v}(2)\gamma^\nu v(4)] \quad (2.2)$$

Similarly for t-channel we have,

$$-i\mathcal{M} = [\bar{u}(3)c_{3k}^\dagger] \left(-i\frac{\alpha_s}{2} \lambda_{ki}^\alpha \gamma^\mu \right) [c_{1i}u(1)] \left(-i\frac{g_{\mu\nu\delta\alpha\beta}}{q^2} \right) [\bar{v}(2)c_{2j}^\dagger] \left(-i\frac{\alpha_s}{2} \lambda_{jl}^\beta \gamma^\nu \right) [c_{4l}v(4)] \quad (2.3)$$

$$\mathcal{M} = \left(\frac{1}{4} c_{3k}^\dagger c_{4l} c_{2j}^\dagger c_{1i} \lambda_{kl}^\alpha \lambda_{ji}^\alpha \right) \left(-\frac{\alpha_s^2}{q^2} \right) [\bar{u}(3) \gamma^\mu u(1)] [\bar{v}(2) \gamma^\nu v(4)] (2\pi)^4 \delta^4(p_1 + p_2 - p_4 - p_3) \quad (2.4)$$

The color factors for t - and s - channels are,

$$f_t = \left(\frac{1}{4} c_{3k}^\dagger c_{4l} c_{2j}^\dagger c_{1i} \lambda_{kl}^\alpha \lambda_{ji}^\alpha \right) \quad f_s = \left(\frac{1}{4} c_{3k}^\dagger c_{4l} c_{2j}^\dagger c_{1i} \lambda_{kl}^\alpha \lambda_{ji}^\alpha \right) \quad (2.5)$$

Since mesons are colorless they are in color singlet state given by,

$$|\text{Meson}\rangle = \frac{1}{\sqrt{3}} (r\bar{r} + b\bar{b} + g\bar{g}) \quad (2.6)$$

therefore,

$$c_{3k}^\dagger c_{4l} c_{2j}^\dagger c_{1i} = \frac{1}{3} \delta_{ij} \delta_{kl} \quad (2.7)$$

Now for s -channel this condition results in,

$$f_s = \frac{1}{12} \sum_{i,j,k,l=1}^3 \sum_{\alpha=1}^8 \delta_{ij} \delta_{kl} \lambda_{kl}^\alpha \lambda_{ji}^\alpha = \frac{1}{12} \sum_{\alpha=1}^8 \text{Tr}[\lambda^\alpha] \text{Tr}[\lambda^\alpha] = 0 \quad (2.8)$$

which says that gluon, as a color octet, do not couple to a meson in color singlet state, this leaves us the t -channel for which the color factor is given as,

$$f_t = \frac{1}{12} \sum_{i,j,k,l=1}^3 \sum_{\alpha=1}^8 \delta_{ij} \delta_{kl} \lambda_{kl}^\alpha \lambda_{ji}^\alpha = \frac{1}{12} \sum_{\alpha=1}^8 \text{Tr}[\lambda^\alpha \lambda^\alpha] = \frac{4}{3} \quad (2.9)$$

Therefore we may conclude that one gluon exchange results in interaction with a Coulomb potential, $V_{q\bar{q}}(r)$, given as,

$$V_{q\bar{q}}(r) = -\frac{4}{3} \frac{\alpha_s}{r} \quad (2.10)$$

2.2 Breit Interaction

In the previous section simplification of one gluon exchange to an interaction via Coulomb potential was enough for showing the attractive nature of the interaction for color singlet states. However a rightful objection can be made that this is an oversimplification because it disregards all the relativistic nature of our problem. In this section we discuss how to include relativistic effects. Naturally when one deals with relativistic bound states, Bethe-Salpeter equation should be used. But for our problem at hand the high masses of charm and beauty quarks allow us to assume that our system can be approximated to be non relativistic. As a

first step in doing a non relativistic reduction, following Breit [9] we attempt to find a non-covariant expression for the scattering amplitude in the form,

$$\mathcal{M}_{NR} = \int \int \Psi^\dagger(\mathbf{p}_3, E_3, j_3; 1) \Psi^\dagger(\mathbf{p}_4, E_4, j_4; 2) \left(\frac{e^2}{r_{12}} + H_B(1, 2) \right) \times \Psi(\mathbf{p}_2, E_2, j_2; 2) \Psi(\mathbf{p}_1, E_1, j_1; 1) d^3 r_1 d^3 r_2 \quad (2.11)$$

where

$$\Psi(\mathbf{p}_i, E_i, j_i; n) = e^{i\mathbf{p}_i \cdot \mathbf{r}_n / \hbar - iE_i t / \hbar} u(n) \quad (2.12)$$

and $H_B(1, 2)$ is the term that includes the relativistic correction. Finding $H_B(1, 2)$ will benefit us in two ways, first it will enable us to find the relativistic correction to the first order and second, by evaluating its expectation value using the wavefunctions that we calculate for $c\bar{c}$ and $b\bar{b}$ mesons will give us an estimation of relativistic effects for our model.

Disregarding the color factor we rewrite the amplitude for one gluon exchange as

$$\mathcal{M} = \frac{1}{(E_1 - E_3)^2 - (\mathbf{p}_1 - \mathbf{p}_3)^2} [\bar{u}(3)\gamma^\mu u(1)] [\bar{v}(2)\gamma^\nu v(4)] \times (2\pi)^4 \delta(E_1 + E_2 - E_4 - E_4) \delta^3(\mathbf{p}_1 + \mathbf{p}_2 - \mathbf{p}_4 - \mathbf{p}_4) \quad (2.13)$$

In terms of α_1, β_1 and α_2, β_2 we can rewrite the the product of the fermion currents as

$$\begin{aligned} [\bar{u}(3)\gamma^\mu u(1)] [\bar{v}(2)\gamma^\nu v(4)] &= [u^\dagger(3)\gamma^0\gamma^\mu u(1)] [v^\dagger(2)\gamma^0\gamma^\nu v(4)] \\ &= [u^\dagger(3)\gamma^0\gamma^\mu u(1)] [v^\dagger(2)\gamma^0\gamma^\nu v(4)] \\ &= u^\dagger(3)v^\dagger(2) (1 - \alpha_1 \cdot \alpha_2) u(1)v(4) \end{aligned} \quad (2.14)$$

where α_1 acts on the spinor space of the first particle and α_2 to that of the second and they commute, so that

$$\mathcal{M} = \frac{1}{(E_1 - E_3)^2 - (\mathbf{p}_1 - \mathbf{p}_3)^2} [u^\dagger(3)v^\dagger(2) (1 - \alpha_1 \cdot \alpha_2) u(1)v(4)] \times (2\pi)^4 \delta(E_1 + E_2 - E_4 - E_4) \delta^3(\mathbf{p}_1 + \mathbf{p}_2 - \mathbf{p}_4 - \mathbf{p}_4) \quad (2.15)$$

Or as an integration over space and time

$$\mathcal{M} = \int \int \int e^{i\mathbf{p}_3 \cdot \mathbf{r}_1 / \hbar} u^\dagger(3) e^{-i\mathbf{p}_2 \cdot \mathbf{r}_2 / \hbar} v^\dagger(2) \left(\frac{1}{r_{12}} (1 - \alpha_1 \cdot \alpha_1) e^{-|E_1 - E_3| r_{12} / \hbar c} \right) \times e^{-i\mathbf{p}_1 \cdot \mathbf{r}_1 / \hbar} u(1) e^{i\mathbf{p}_4 \cdot \mathbf{r}_1 / \hbar} v(4) e^{i(E_1 + E_2 - E_3 - E_4)t / \hbar} d^3 r_1 d^3 r_2 dt \quad (2.16)$$

Now using

$$e^{-i/\hbar(E_n t_1 - \mathbf{p}_n \cdot \mathbf{r}_1)} u(n) = \Psi_n(\mathbf{p}_n, E_n, j_i) \quad (2.17)$$

$$e^{i/\hbar(E_n t_2 - \mathbf{p}_n \cdot \mathbf{r}_2)} v(n) = \Psi_n(-\mathbf{p}_n, -E_n, j_n; n) \quad (2.18)$$

We obtain

$$\mathcal{M}_R = \int \int \Psi^\dagger(\mathbf{p}_3, E_3) \Psi^\dagger(-\mathbf{p}_2, E_2) \left\{ \frac{1}{r_{12}} (1 - \alpha_1 \cdot \alpha_1) e^{-|E_1 - E_3| r_{12} / \hbar c} \right\} \times \Psi(\mathbf{p}_1, E_1) \Psi(-\mathbf{p}_4, -E_4) d^3 r_1 d^3 r_2 \quad (2.19)$$

To obtain the non-relativistic reduction of the amplitude \mathcal{M}_R which we assume is of the form \mathcal{M}_{NR} given in Eqn.[2.11], we observe that for one gluon exchange we are at short distances which are characterized by high momentum exchange $|\mathbf{p}_1 - \mathbf{p}_3|$, quantitatively we may associate the distance between $q\bar{q}$ pair to de Broglie wavelength [13],

$$r_{12} \approx \hbar / |\mathbf{p}_1 - \mathbf{p}_3| \quad (2.20)$$

Therefore the exponential in Eqn.[2.19] is at the order

$$e^{-|E_1 - E_3| r_{12} / \hbar c} = e^{-|E_1 - E_3| / |\mathbf{p}_1 - \mathbf{p}_3| c} \quad (2.21)$$

For the system we are concerned with the quark masses are at the order of GeV, therefore the exponent can be approximated as, $|E_1 - E_3| / |\mathbf{p}_1 - \mathbf{p}_3| c \approx (\mathbf{p}_1^2 - \mathbf{p}_3^2) / m^2 c^3 |\mathbf{p}_1 - \mathbf{p}_3| \lll 1$. Where we have used $E = \sqrt{\mathbf{p}^2 + m^2} \approx m + \mathbf{p}^2 / 2m$, since we assume quark masses to be high. Using this assumption we expand the term in the curly brackets in Eqn.[2.19],

$$\frac{1}{r_{12}} (1 - \alpha_1 \cdot \alpha_1) e^{-|E_1 - E_3| r_{12} / \hbar c} = \frac{1}{r_{12}} (1 - \alpha_1 \cdot \alpha_2) \quad (2.22)$$

$$\times \left(1 + i \frac{|E_3 - E_1| r_{12}}{c \hbar} - \frac{|E_3 - E_1|^2 r_{12}^2}{(c \hbar)^2} + \dots \right) = \frac{1}{r_{12}} - \frac{\alpha_1 \cdot \alpha_2}{r_{12}} + i \frac{|E_3 - E_1|}{c \hbar} - \frac{|E_3 - E_1|^2 r_{12}}{2(c \hbar)^2} + \dots \quad (2.23)$$

The first term is just the Coulomb potential, the second term

$$H_{B,m} = -\frac{\alpha_1 \cdot \alpha_2}{r_{12}} \quad (2.24)$$

is called the Breit magnetic term and its physical meaning is explained below. The third term, $i\frac{|E_3-E_1|}{c\hbar}$, does not have any dependence on r_{12} therefore for this term the integrals over r_1 and r_2 can be carried out separately to give zero, since the incoming and outgoing waves are considered to be orthogonal.

To find the contribution from the fourth term first we note that, since $(E_3 - E_1) = (E_2 - E_4)$,

$$-\frac{|E_3 - E_1|^2 r_{12}}{2(c\hbar)^2} = -\frac{(E_3 - E_1)(E_2 - E_4)r_{12}}{2(c\hbar)^2} \quad (2.25)$$

$$= -(E_3E_2 + E_1E_4 - E_1E_2 - E_3E_4)\frac{r_{12}}{2(c\hbar)^2} \quad (2.26)$$

Therefore the contribution is

$$M_{B,ret} = -\frac{1}{2} \int \int \int \Psi^\dagger(\mathbf{p}_3, E_3)\Psi^\dagger(-\mathbf{p}_2, -E_2) \quad (2.27)$$

$$\times \left\{ \frac{r_{12}}{(c\hbar)^2} (E_3E_2 + E_1E_4 - E_1E_2 - E_3E_4) \right\} \quad (2.28)$$

$$\times \Psi(\mathbf{p}_1, E_1)\Psi(-\mathbf{p}_4, -E_4)d^3r_1d^3r_2dt \quad (2.29)$$

To extract the Hamiltonian we need to replace energies with their operator form. Using

$$(i\hbar\alpha_i \cdot \nabla_i + \beta_i m)\Psi_n(\mathbf{p}_n, E_n) = E_n\Psi_n(\mathbf{p}_n, E_n) \quad (2.30)$$

where $i = 1(2)$ for $n = 1, 3, (2, 4)$, we express the product of energies as

$$\begin{aligned} \Psi^\dagger(\mathbf{p}_3, E_3)\Psi^\dagger(-\mathbf{p}_2, -E_2)\frac{r_{12}}{(c\hbar)^2}(E_3E_2) &= \Psi^\dagger(\mathbf{p}_3, E_3)\Psi^\dagger(-\mathbf{p}_2, -E_2)(-i\hbar\alpha_1 \cdot \nabla_1 + \beta_1 m) \\ &= \times(-i\hbar\alpha_2 \cdot \nabla_2 + \beta_2 m)\frac{r_{12}}{(c\hbar)^2} \end{aligned} \quad (2.31)$$

$$\begin{aligned} \frac{r_{12}}{(c\hbar)^2}(E_1E_4)\Psi(\mathbf{p}_1, E_1)\Psi(-\mathbf{p}_4, -E_4) &= \frac{r_{12}}{(c\hbar)^2}(i\hbar\alpha_1 \cdot \nabla_1 + \beta_1 m)(i\hbar\alpha_2 \cdot \nabla_2 + \beta_2 m) \\ &\times \Psi(\mathbf{p}_1, E_1)\Psi(-\mathbf{p}_4, -E_4) \end{aligned} \quad (2.32)$$

$$\begin{aligned} -\Psi^\dagger(-\mathbf{p}_2, -E_2)\Psi(\mathbf{p}_1, E_1)\frac{r_{12}}{(c\hbar)^2}(E_1E_2) &= -\Psi^\dagger(-\mathbf{p}_2, -E_2)(-i\hbar\alpha_2 \cdot \nabla_2 + \beta_2 m)\frac{r_{12}}{(c\hbar)^2} \\ &\times (i\hbar\alpha_1 \cdot \nabla_1 + \beta_1 m)\Psi(\mathbf{p}_1, E_1) \end{aligned} \quad (2.33)$$

$$\begin{aligned} -\Psi^\dagger(-\mathbf{p}_3, -E_3)\Psi(\mathbf{p}_4, E_4)\frac{r_{12}}{(c\hbar)^2}(E_3E_4) &= -\Psi^\dagger(-\mathbf{p}_3, -E_3)(-i\hbar\alpha_1 \cdot \nabla_1 + \beta_1 m)\frac{r_{12}}{(c\hbar)^2} \\ &\times (i\hbar\alpha_2 \cdot \nabla_2 + \beta_2 m)\Psi(\mathbf{p}_4, E_4) \end{aligned} \quad (2.34)$$

Observing that, since $\beta_{1,2}$ commute with r_{12} , the terms with $\beta_1\beta_2r_{12}$ and $\beta\alpha \cdot \nabla$ cancel out, resulting in,

$$\begin{aligned}
M_{B,ret} = & -\frac{1}{2} \int \int \int \Psi^\dagger(\mathbf{p}_3, E_3) \Psi^\dagger(-\mathbf{p}_2, -E_2) \\
& \times \{-\alpha_1 \cdot \nabla_1 \alpha_2 \cdot \nabla_2 r_{12} - r_{12} \alpha_1 \cdot \nabla_1 \alpha_2 \cdot \nabla_2 + \alpha_1 \cdot \nabla_1 r_{12} \alpha_2 \cdot \nabla_2 + \alpha_2 \cdot \nabla_2 r_{12} \alpha_1 \cdot \nabla_1\} \\
& \times \Psi(\mathbf{p}_1, E_1) \Psi(-\mathbf{p}_4, -E_4) d^3 r_1 d^3 r_2 dt
\end{aligned} \tag{2.35}$$

The term in the curly brackets can be evaluated using,

$$\begin{aligned}
-\alpha_1 \cdot \nabla_1 \alpha_2 \cdot \nabla_2 r_{12} &= -\alpha_1 \cdot \nabla_1 (\alpha_2 \cdot r_{12} \nabla_2 + \nabla_2 r_{12}) \\
&= -r_{12} \alpha_1 \cdot \nabla_1 \alpha_2 \cdot \nabla_2 - \alpha_1 \cdot \nabla_1 (r_{12}) \alpha_2 \cdot \nabla_2 \\
&\quad - (\alpha_1 \cdot \nabla_1) (\alpha_2 \cdot \nabla_2) (r_{12}) - \alpha_2 \cdot \nabla_2 (r_{12}) \alpha_1 \cdot \nabla_1
\end{aligned} \tag{2.36}$$

$$\alpha_1 \cdot \nabla_1 r_{12} \alpha_2 \cdot \nabla_2 = r_{12} \alpha_1 \cdot \nabla_1 \alpha_2 \cdot \nabla_2 + \alpha_1 \cdot \nabla_1 (r_{12}) \alpha_2 \cdot \nabla_2 \tag{2.37}$$

$$\alpha_2 \cdot \nabla_2 r_{12} \alpha_1 \cdot \nabla_1 = r_{12} \alpha_2 \cdot \nabla_2 \alpha_1 \cdot \nabla_1 + \alpha_2 \cdot \nabla_2 (r_{12}) \alpha_1 \cdot \nabla_1 \tag{2.38}$$

Putting everything together we obtain,

$$M_{B,ret} = -\frac{1}{2} \int \int \int \Psi^\dagger(\mathbf{p}_3, E_3) \Psi^\dagger(-\mathbf{p}_2, -E_2) (\alpha_1 \cdot \nabla_1) (\alpha_2 \cdot \nabla_2) (r_{12}) \tag{2.39}$$

$$\times \Psi(\mathbf{p}_1, E_1) \Psi(-\mathbf{p}_4, -E_4) d^3 r_1 d^3 r_2 dt \tag{2.40}$$

Allowing us to identify the operator responsible for the retardation effect,

$$H_{B,ret} = -\frac{1}{2} (\alpha_1 \cdot \nabla_1) (\alpha_2 \cdot \nabla_2) (r_{12}) \tag{2.41}$$

Which together with 2.24, gives the Breit operator,

$$H_{Breit} = -\frac{\alpha_1 \cdot \alpha_2}{r_{12}} + \frac{1}{2} (\alpha_1 \cdot \nabla_1) (\alpha_2 \cdot \nabla_2) (r_{12}) \tag{2.42}$$

Or,

$$H_{Breit} = -\frac{1}{2} \left[\frac{\alpha_1 \cdot \alpha_2}{r_{12}} + \frac{(\alpha_1 \cdot \mathbf{r}_{12})(\alpha_2 \cdot \mathbf{r}_{12})}{r_{12}^3} \right] \quad (2.43)$$

Therefore if one considers the lowest order relativistic corrections to one-gluon exchange, the relativistic Hamiltonian for the quark-anti-quark system may be given as,

$$H = c\alpha_1 \cdot p_1 + c\alpha_2 \cdot p_2 + \beta_1 mc^2 + \beta_2 mc^2 - \frac{1}{r_{12}} - \frac{1}{2} \left[\frac{\alpha_1 \cdot \alpha_2}{r_{12}} + \frac{(\alpha_1 \cdot \mathbf{r}_{12})(\alpha_2 \cdot \mathbf{r}_{12})}{r_{12}^3} \right] \quad (2.44)$$

2.3 Potential Model

2.3.1 The Cornell Potential

As mentioned before Quark Model needs to embrace both the non-perturbative and perturbative regimes of QCD. As shown in the previous section, in perturbative regime, where coupling is small we only need to consider one gluon exchange which, ignoring the color factor, is just a Coulomb potential for color singlet states,

$$V_{1g}(r) = -\frac{4}{3} \frac{\alpha_s}{r} \quad (2.45)$$

To account for the non-perturbative regime, different potential models have been proposed in the early days of the quark model, most notable ones are the logarithmic potential $\ln(r)$ and power-law potential, r^ν [37]. Today, with the results from Lattice QCD, Wilson Loop Calculations and Effective Field Theory approach we expect that confining potential should be linear,

$$V_{Conf}(r) = \sigma r \quad (2.46)$$

The resulting phenomenological potential together with constant term V_0 ,

$$V_{Cornell} = -\frac{4}{3} \frac{\alpha_s}{r} + \sigma r + V_0 \quad (2.47)$$

is called the Cornell potential, where V_0 is a constant. Although at first sight adding a constant term may seem illegal, we note that there is no counter argument for such a term, and there is no harm in including it except increasing parameters.

2.3.2 Breit-Fermi Interactions

Cornell potential on its own is unfortunately unable to explain spin splittings, such as J/Ψ and η_c , and P wave splittings such as $\chi_{c0}, \chi_{c1}, \chi_{c2}, h_c$. To include these splittings we have to include spin-dependent terms to the potential.

As it is clear now we face two different energy regimes and we have no clue from the theory about how the spin dependent forces change with the distance. As shown in [14] hypothesizing that the spin-dependent forces are attributed to the short distance potential, one can explain the observed Hadron masses to a high precision. Also from [17], [18] and [44] Cornell potentials success in building a model for Charmonium can be observed.

In this section we show how to obtain the the spin dependent potentials following the assumption that it results from the 1-gluon exchange. In the previous section we have already found a non-covariant Dirac Hamiltonian which included retardation effects. As it is a relativistic Hamiltonian it is spin dependent and it mixes negative and positive energy solutions. To use this Hamiltonian in our non-relativistic model we can remove such a mixing by making a non relativistic reduction which in turn will allow us to separate spin and space parts of the wavefunction, providing us with spin dependent forces occurring at higher orders of $1/m$.

Such a non-relativistic reduction is made in Appendix A, by using generalized Foldy-Wouthuysen transformation for two particles. The result of non-relativistic expansion to order $1/m^3$ is given as,

$$H_{BF} = -\frac{4}{3} \frac{\alpha_s}{r} \quad (2.48)$$

$$+2m_q + \frac{\mathbf{p}^2}{m_q} - \frac{\mathbf{p}^4}{4m_q^3} \quad (2.49)$$

$$-\frac{2}{3} \frac{\alpha_s}{m_q^2} \left(\frac{\mathbf{p}^2}{r} + \frac{\mathbf{r}(\mathbf{r} \cdot \mathbf{p}) \cdot \mathbf{p}}{r^3} \right) \quad (2.50)$$

$$+\frac{4}{3} \frac{\alpha_s}{m_q^2} \delta(\mathbf{r}) \left(1 + \frac{8\pi}{3} \mathbf{S}_1 \cdot \mathbf{S}_2 \right) \quad (2.51)$$

$$+2 \frac{\alpha_s}{m_q^2 r^3} ((\mathbf{S}_1 + \mathbf{S}_2) \cdot \mathbf{L}) \quad (2.52)$$

$$+\frac{4}{3} \frac{\alpha_s}{m_q^2 r^3} \left(3 \frac{(\mathbf{S}_1 \cdot \mathbf{r})(\mathbf{S}_2 \cdot \mathbf{r})}{r^2} - \mathbf{S}_1 \cdot \mathbf{S}_2 \right) \quad (2.53)$$

We know put the Breit interaction, term by term in a form suitable for our method of using the radial solutions of the Harmonic Oscillator and give the explanation of each term.

2.3.2.1 Increase of Relativistic Mass

Eqn [2.49] corresponds the expansion of $2 \sqrt{\mathbf{p}^2 + m_q^2}$.

$$V_{rm} = 2m + \frac{\mathbf{p}^2}{m} - \frac{\mathbf{p}^4}{4m^3} \quad (2.54)$$

Such a term arises when one considers the relativistic mass, γm_0 instead of the rest mass m_0 . In our model we are only interested in terms contributing to the the order m^2 therefore we discard the term $-\frac{\mathbf{p}^4}{4m^3}$ and use

$$2m_q + \frac{\mathbf{p}^2}{m_q} \quad (2.55)$$

instead, which corresponds to the Schrodinger Hamiltonian without a potential.

2.3.2.2 Retardation of Potential

Eqn (2.50), as explained in detail in the previous section arises from the retardation of the potential resulting from the finite speed of propagation of light (gluons in our case). In operator

form it is given as

$$\begin{aligned}
\langle \Psi_{nlm}(\mathbf{r}) | V_{ret} | \Psi_{n'l'm'}(\mathbf{r}) \rangle &= \left\{ -\frac{2}{3} \frac{\alpha_s}{m_q^2} \int r^2 dr R_n \left(\frac{\nabla^2}{r} + \frac{1}{r} \frac{\partial^2}{\partial r^2} \right) R_{n'} \int d\Omega Y_{lm}^* Y_{l'm'} \right. \\
&\quad \left. + \int r^2 dr R_n R_{n'} \int d\Omega Y_{lm}^* \frac{\nabla^2}{r} Y_{l'm'} \right\} \quad (2.56) \\
&= -\frac{2}{3} \frac{\alpha_s}{m_q^2} \int dr \left\{ \frac{2}{r} u_{n'} u_n'' - \frac{2}{r^2} u_{n'} u_n' + \frac{2-l(l+1)}{r^3} u_n u_{n'} \right\} \\
&\quad \times \delta_{mm'} \delta_{ll'}
\end{aligned}$$

Note that we use the radial solutions of the harmonic oscillator but the above term also acts on the angular part. We separate the angular dependency as follows,

$$\begin{aligned}
\langle \Psi_{nlm}(\mathbf{r}) | V_{ret} | \Psi_{n'l'm'}(\mathbf{r}) \rangle &= \left\{ -\frac{2}{3} \frac{\alpha_s}{m_q^2} \int r^2 dr R_n \left(\frac{\nabla^2}{r} + \frac{1}{r} \frac{\partial^2}{\partial r^2} \right) R_{n'} \int d\Omega Y_{lm}^* Y_{l'm'} \right. \\
&\quad \left. + \int r^2 dr R_n R_{n'} \int d\Omega Y_{lm}^* \frac{\nabla^2}{r} Y_{l'm'} \right\} \quad (2.57) \\
&= -\frac{2}{3} \frac{\alpha_s}{m_q^2} \int dr \left(\frac{2}{r} u_{n'} u_n'' - \frac{2}{r^2} u_{n'} u_n' + \frac{2-l(l+1)}{r^3} u_n u_{n'} \right) \delta_{mm'} \delta_{ll'}
\end{aligned}$$

2.3.2.3 Darwin Term

The first term in Eq.(2.51) ,

$$V_{Darwin} = \frac{4}{3} \frac{\alpha_s}{m_q^2} \delta(\mathbf{r}) \quad (2.58)$$

is called the Darwin term and may be attributed zitterbewegung [5]. It is a correction that includes the smearing out of the potential caused by the fluctuation of the particle, quark and anti-quark in this case, over the distance $\delta r \approx 1/m_q$. The smearing may be approximated as,

$$\langle \delta V \rangle = \langle V(\mathbf{r} + \delta \mathbf{r}) \rangle - \langle V(\mathbf{r}) \rangle = \left\langle \delta r \frac{\partial V}{\partial r} + \delta r_i \delta r_j \frac{\partial^2 V}{\partial r_i \partial r_j} \right\rangle \approx \frac{1}{6} \delta r^2 \nabla^2 V \approx \frac{1}{6m^2} \nabla^2 V \quad (2.59)$$

To include this term in our Hamiltonian, we write Dirac Delta function in spherical coordinates,

$$V_{Darwin} = \frac{4}{3} \frac{\alpha_s}{m_q^2} \delta(\mathbf{r}) = \frac{4}{3} \frac{\alpha_s}{m_q^2} \frac{\delta(r)}{2\pi r^2} \quad (2.60)$$

by noting that $1 = \int dr r^2 R_{nl}(r) \int d\Omega Y_{lm}(\theta, \phi) = (4\pi) \int dr r^2 R_{nl}(r)$, and that the integration is from 0^+ to ∞ . Obviously this term only contributes only for $l = 0$ states for which there is no centrifugal potential, and radial wavefunction R_{nl} is non-zero at the origin.

2.3.2.4 Spin-Spin Interaction

The spin-spin interaction term,

$$\frac{4}{3} \frac{\alpha_s}{m_q^2} \delta(\mathbf{r}) \left(\frac{8\pi}{3} \mathbf{S}_1 \cdot \mathbf{S}_2 \right) \quad (2.61)$$

arises when one considers two particles. Together with the regular Spin-Spin interaction its presence is vital in explaining the S wave splittings. Note that it has no effect for $l \neq 0$ states. In $|j, l, s, m_j\rangle$ basis it is given as

$$V_{SS,con} = \frac{16}{9} \frac{\alpha_s}{m_q^2} \frac{\delta(r)}{r^2} \left(S(S+1) - \frac{3}{2} \right) \quad (2.62)$$

where we have used $\mathbf{S}_1 \cdot \mathbf{S}_2 = \frac{1}{2}(\mathbf{S}^2 - \mathbf{S}_1^2 - \mathbf{S}_2^2) = \frac{1}{2}(S(S+1) - \frac{3}{2})$.

2.3.2.5 Spin-Orbit Coupling

The spin-orbit coupling term is responsible for P wave splittings and given as,

$$V_{SO}(r) = 2 \frac{\alpha_s}{m_q^2 r^3} (3(\mathbf{S}_1 + \mathbf{S}_2) \cdot \mathbf{L}) \quad (2.63)$$

$$= \frac{\alpha_s}{m_q^2 r^3} (J(J+1) - L(L+1) - S(S+1)) \quad (2.64)$$

where we have used

$$\begin{aligned} \vec{L} \cdot \vec{S} &= \frac{1}{2} \left((\vec{L} + \vec{S})^2 - \vec{L}^2 - \vec{S}^2 \right) \\ &= \frac{1}{2} \left((\vec{J})^2 - \vec{L}^2 - \vec{S}^2 \right) \\ &= \frac{1}{2} (J(J+1) - L(L+1) - S(S+1)) \end{aligned}$$

2.3.2.6 Tensor Force

The tensor potential is given as

$$V_{Tensor} = \frac{4}{3} \frac{\alpha_s}{m_q^2 r^3} \left(3 \frac{(\mathbf{S}_1 \cdot \mathbf{r})(\mathbf{S}_2 \cdot \mathbf{r})}{r^2} - \mathbf{S}_1 \cdot \mathbf{S}_2 \right) \quad (2.65)$$

It is vital in explaining the non-uniformity of the splittings between $L = 1, S = 1$ states such as χ_{c2}, χ_{c1} and χ_{c0} . In $|j, l, s, m_j\rangle$ basis its given as (see Appendix B for Derivation),

$$T_{Tensor} = 3 \frac{(\vec{S}_i \cdot r)(\vec{S}_j \cdot r)}{r^2} - \vec{S}_i \cdot \vec{S}_j = \begin{cases} -\frac{l}{2(2l+3)} & j = l + 1 \\ 1/2 & j = l \\ -\frac{(l+1)}{2(2l-1)} & j = l - 1 \\ 0 & l = 0 \text{ or } s = 0 \end{cases} \quad (2.66)$$

where

$$V_{Tensor}(r, j, l, s) = \frac{4}{3} \frac{\alpha_s}{m_q^2 r^3} T_{tensor}(j, l, s) \quad (2.67)$$

CHAPTER 3

METHOD

3.1 Schrödinger Equation with Central Potential

The fundamental assumption of the quark model is that the constituent quarks obey the non-relativistic Schrodinger equation. Under this assumption we find the non-relativistic reduction of the Breit Hamiltonian using a Foldy Wouthuysen transformation (details are in Appendix A). This reduction allows us to separate the spin and space parts of the meson wavefunction where space part of the wavefunction satisfies the Schrodinger equation with spin dependent potential.

To analyze the motion we start with the Hamiltonian for two particles interacting through an isotropic potential and separate the motion of center of mass,

$$H = \frac{\mathbf{p}_1^2}{2} + \frac{\mathbf{p}_2^2}{2} + V_0(|\mathbf{r}_1 - \mathbf{r}_2|) = \frac{\mathbf{P}^2}{2(m_1 + m_2)} + \frac{\mathbf{p}^2}{2\mu} + V_0(|\vec{\mathbf{r}}|) = H_{CM} + H_{rel} \quad (3.1)$$

where

$$\begin{aligned} \mathbf{P} &= \mathbf{p}_1 + \mathbf{p}_2, \mathbf{p} = \frac{(m_2\mathbf{p}_1 - m_1\mathbf{p}_2)}{m_1 + m_2} \\ \mathbf{r} &= \mathbf{r}_1 + \mathbf{r}_2, \mu = \frac{m_1m_2}{m_1 + m_2} \\ H_{CM} &= \frac{\mathbf{P}^2}{2(m_1 + m_2)}, H_{rel} = \frac{\mathbf{p}^2}{2\mu} \end{aligned}$$

Substituting $\vec{p} \rightarrow -i\vec{\nabla}$ in the Hamiltonian for the relative motion we find the Schrodinger equation,

$$\left[-\frac{\nabla^2}{2\mu} + V_0(r)\Psi(\mathbf{r}) \right] = E\Psi(\mathbf{r}) \quad (3.2)$$

Next we separate the wavefunction into radial and angular parts,

$$\Psi(\vec{r}) = R_{kl}(r)Y_{lm}(\theta, \phi) \quad (3.3)$$

Radial part satisfies

$$\left[-\frac{1}{2\mu} \frac{\partial^2}{\partial r^2} + \frac{2}{r} \frac{\partial}{\partial r} + \frac{l(l+1)}{2\mu r^2} + V_0(r) \right] R_{kl}(r) = E_{kl} R_{kl}(r) \quad (3.4)$$

whereas the angular wavefunctions given in terms of spherical harmonics,

$$Y_{lm}(\theta, \phi) = \epsilon \sqrt{\frac{(2l+1)(l-|m|)!}{4\pi(l+|m|)!}} e^{im\phi} P_l^m(\cos\theta) \quad (3.5)$$

where $\epsilon = (-1)^m$ for $m \geq 0$ and $\epsilon = 1$ for $m \leq 0$.

Defining $u_{kl}(r) = rR_{kl}(r)$, the radial equation simplifies to the 1 dimensional case with effective potential,

$$\left[-\frac{1}{2\mu} \partial_r^2 + \frac{l(l+1)}{2\mu r^2} + V_0(r) \right] u_{kl}(r) = E_{kl} u_{kl}(r) \quad (3.6)$$

The normalization conditions are given as,

$$\int dr r^2 [R_{kl}(r)]^2 = \int dr [u_{kl}(r)]^2 = 1 \quad (3.7)$$

$$\int d\Omega |Y_{lm}(\theta, \phi)|^2 = 1 \quad (3.8)$$

3.1.1 Simple Harmonic Oscillator in Three Dimensions

We will use the radial solutions of isotropic simple harmonic oscillator in three dimensions as our base space to diagonalize the Hamiltonian. The radial part of the 3D SHO wavefunction satisfies,

$$\left(-\frac{1}{2} \nabla^2 + \frac{v^2}{\mu} r^2 - E_n \right) R_{SHO;nl} = 0 \quad (3.9)$$

and the radial equation is given as,

$$R_{SHO;nl}(r, v) = N_{nl} r^l e^{-vr^2} L_{\frac{n-l}{2}}^{(l+\frac{1}{2})}(2vr^2) \quad (3.10)$$

where μ is the reduced mass and,

$$N_{nl} = \sqrt{\sqrt{\frac{2v^3}{\pi} \frac{2\left(\frac{n-l}{2}\right)! v^l}{\left(\frac{n+l}{2} + 1\right)!!}} \quad (3.11)$$

ensures normalization. $L_{\frac{n-l}{2}}^{(l+\frac{1}{2})}(2vr^2)$ are generalized Laguerre polynomials. The quantum number n denotes the energy values.

$$E_{3DSHO} = \hbar\omega \left(n + \frac{3}{2} \right) \quad (3.12)$$

l denotes the total angular momentum. $\frac{n-l}{2} = k$ gives the radial quantum number and is an integer. Therefore n can have the values

$$n = 0, 1, 2, \dots$$

and l can have,

$$l = \begin{cases} 0, 2, 4, \dots, n & \text{for } n \text{ even} \\ 1, 2, 3, \dots, n & \text{for } n \text{ odd} \end{cases}$$

ν is the parameter of wave function depending on the angular frequency of the harmonic oscillator. We will fix this parameter by considering a perturbation,

$$\delta V = kx - \mu\omega^2 r^2 \quad (3.13)$$

to the Hamiltonian given in 3.9. The first order correction to the ground state is given as,

$$\langle u_{SHO;0} | \delta V | u_{SHO;0} \rangle = \frac{4k \sqrt{\frac{2}{\pi}}}{3 \sqrt{\nu}} - \frac{5m\omega^2}{8\nu} \quad (3.14)$$

Now we demand this perturbation to vanish, obtaining

$$\nu_0 = \frac{4k^{2/3} \mu^{2/3}}{15^{2/3} \pi^{1/3}} \quad (3.15)$$

At this stage the basis vectors are given by,

$$u_{SHO;n} \equiv r R_{SHO;n}(r, \nu_0) = N_{nl} r^{l+1} e^{-\nu r^2} L_{\frac{n-l}{2}}^{(l+\frac{1}{2})}(2\nu_0 r^2) \quad (3.16)$$

3.1.2 Method

To summarize we use the 3D SHO reduced radial wavefunctions,

$$u_{SHO;n}(r, \nu) = N_{nl} r^{l+1} e^{-\nu r^2} L_{\frac{n-l}{2}}^{(l+\frac{1}{2})}(2\nu r^2) \quad (3.17)$$

to diagonalize the Hamiltonian given as

$$\begin{aligned}
H = & -\frac{1}{m_q} \frac{\partial^2}{\partial^2 r} + \frac{l(l+1)}{m_q r^2} \\
& -\frac{4\alpha_s}{3r} + \sigma r \\
& +2m_q + \frac{\mathbf{p}^2}{m_q} \\
& -\frac{2\alpha_s}{3m_q^2} \left(\frac{\nabla^2}{r} + \frac{1}{r} \frac{\partial}{\partial r} \right) \\
& +\frac{4\alpha_s}{3m_q^2} \frac{\delta(r)}{2\pi r^2} \left(1 + \frac{4\pi}{3} \frac{\delta(r)}{r^2} \left(S(S+1) - \frac{3}{2} \right) \right) \\
& +\frac{\alpha_s}{m_q^2 r^3} (J(J+1) - L(L+1) - S(S+1)) \\
& +\frac{4}{3} \frac{\alpha_s}{m_q^2 r^3} T_{tensor}(j, l, s)
\end{aligned} \tag{3.18}$$

Obtaining,

$$Hu_{q\bar{q};k,j,l,s}(r) = E_{n;j,l,s} u_{q\bar{q};k,j,l,s}(r) \tag{3.19}$$

where $u_{q\bar{q};k,j,l,s}(r)$ is the reduced radial wavefunction of the meson, i.e.,

$$u_{q\bar{q};k,j,l,s}(r) \equiv rR_{q\bar{q};k,j,l,s}(r) \tag{3.20}$$

and is given by in terms of 3D SHO reduced wavefunctions as,

$$u_{q\bar{q};k,j,l,s}(r) = \begin{cases} \sum_{n=l}^{2D-2} c_n u_{SHO;n,l} & \text{for } l = \text{even} \\ \sum_{n=l}^{l+2D-2} c_n u_{SHO;n,l} & \text{for } l = \text{odd} \end{cases} \tag{3.21}$$

Where D is the number of the SHO wavefunctions forming the base space, i.e. the dimension of the Hamiltonian matrix that we diagonalize. And the mass of the meson is found by adding the two times the mass of quark to the eigenenergy,

$$M_{k,j,l,s} = 2m_q + E_{k;j,l,s} \tag{3.22}$$

To find the fitting parameters, (α_s, k, m_q) we define,

$$\chi^2(\alpha_s, k, m_q) = \Sigma \frac{(M_{exp,k,j,l,s} - M_{k,j,l,s})^2}{\Delta M_{exp,k,j,l,s}} \tag{3.23}$$

Where $M_{exp,n,j,l,s}$ is the experimental observations of the meson masses and $\Delta M_{exp,n,j,l,s}$ is the error in measurements. Using Mathematica, the parameters (α_s, k, m_q) are fixed so that χ^2 is

a minimum. The dimension of the base space is chosen to be 30. Convergence is observed by considering base spaces with different dimensions.

CHAPTER 4

SPECTRUM AND RADIATIVE TRANSITIONS

4.1 Charmonium

Using the method described above we fit the parameters as

$$\begin{array}{ccc} \alpha_s & \sigma & m_c \\ 0.3864 & 0.2192\text{GeV}^2 & 1.260\text{GeV} \end{array} \quad (4.1)$$

The predicted spectrum for Charmonium is given in Table 1. We also plot the ground state and first excited state wavefunctions. In [28] the mass of the charm quark is given between 1.18 GeV-1.34 GeV, and our mass value lies inside this range. Also the fitted σ is above the results obtained from lattice simulations which is around $\sigma_{lattice} \approx 0.15 \text{ GeV}^2$ [30]. The value we obtained for α_s is only half the value of that obtained for Charmonium from lattice calculations, which is around 0.65.

Comparing the found mass spectrum with the experimental results we see that our model for describing the 1S splitting is not as much as successful as we would like it to be, considering we only use 1S and 1P results for the fit.

For excited states we see that our calculations give increasingly higher mass. This might be attributed to the closeness of this state to $D - \bar{D}$ threshold.

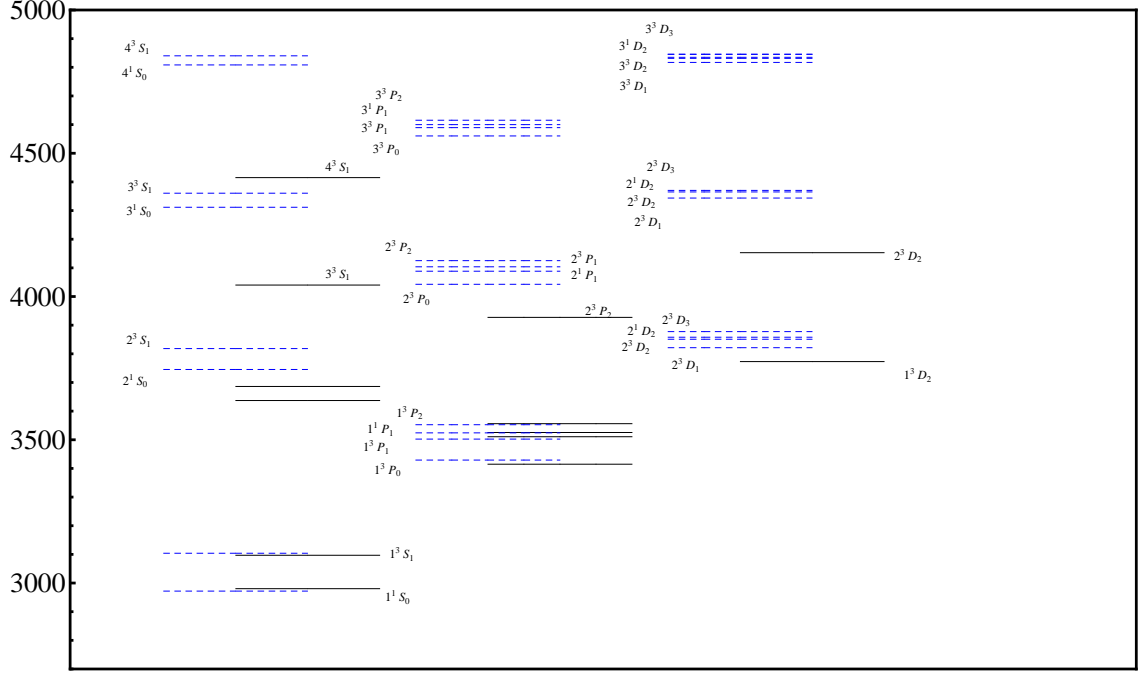


Figure 4.1: Charmonium Spectrum Showing Experimental Measurements(Black) vs. Fitted Mass Values (Blue, dotted).

4.2 Bottomonium

For the Bottomonium we fit the parameters as,

$$\begin{array}{ccc}
 \alpha_s & \sigma & m_b \\
 0.3262 & 0.2902\text{GeV} & 4.630
 \end{array} \tag{4.2}$$

The predicted spectrum is given in Table 2. We also plot the ground state and first excited state wavefunctions. In [28] the mass of the bottom quark is given between $(4.49 - 4.61)\text{GeV}$, our fitted mass is slightly above this range. σ is found to be above the lattice predictions $\sigma_{lattice} \approx 0.15 \text{ GeV}^2$. One expects the string tension to remain the same for different flavors but our model fails to predict this property, this may be attributed to the failure of the fit for Charmonium spectra. Compared to Charmonium a smaller value for α_s is obtained. This is in agreement with the asymptotic freedom, since as we can observe from the graph the radial wavefunctions are packed closer to the origin, meaning a larger value for the momentum exchange therefore a smaller value for the α_s .

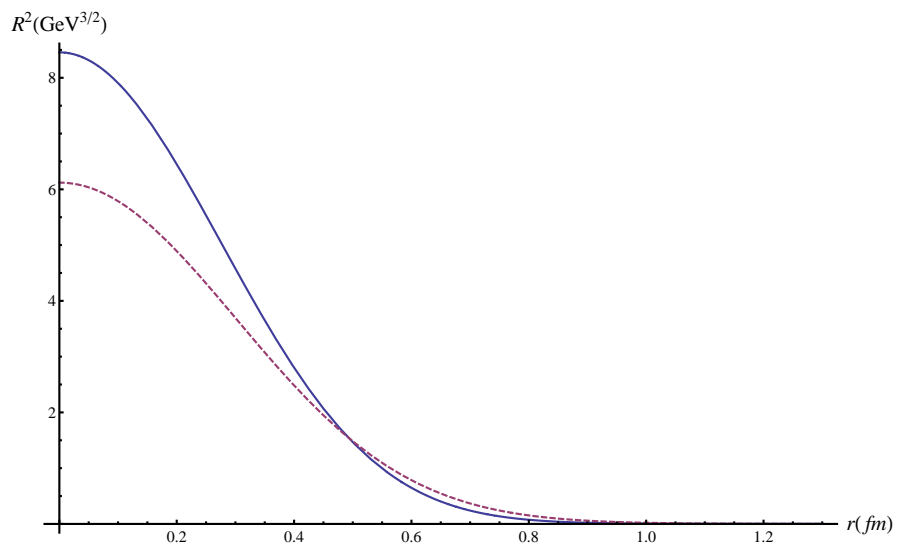


Figure 4.2: Squared radial wavefunctions for η_c (blue straight) and J/ψ (red dashed)

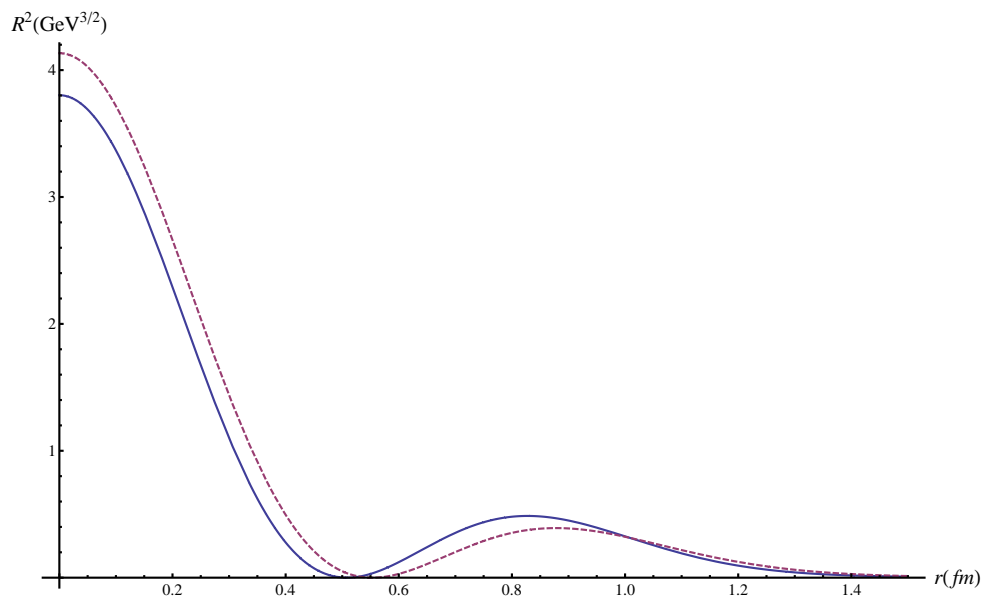


Figure 4.3: Squared radial wavefunctions for $\eta_c(2S)$ (blue straight) and $J/\psi(2S)$ (red dashed).

Table 4.1: Calculated and experimental values, [28], of $c\bar{c}$ and $b\bar{b}$ spectra. The dagger shows which states are used for the fit

State	Charmonium			Bottomonium		
	Meson	Experiment (MeV)	Fit (MeV)	Meson	Experiment (MeV)	Fit (MeV)
1^1S_0	η_c^\dagger	2980.3 ± 1.2	2972	η_b^\dagger	9390.9 ± 2.8	9391
1^3S_1	J/ψ^\dagger	3096.916 ± 0.011	3104	$\Upsilon(1S)^\dagger$	9460.30 ± 0.26	9460
2^1S_0	$\eta_c(2S)$	3637 ± 4	3745			10069
2^3S_1	$\psi(2S)$	3686.09 ± 0.04	3818	$\Upsilon(2S)$	$10\,023.26 \pm 0.31$	10101
3^1S_0			4312			10523
3^3S_1	$\psi(4040)$	3772.92 ± 0.35	4361	$\Upsilon(3S)$	$10\,355.2 \pm 0.5$	10546
4^1S_0			4808			10905
4^3S_1	$\psi(4415)$	4421 ± 4	4840	$\Upsilon(4S)$	$10\,579.4 \pm 1.2$	10922
1^3P_2	χ_{c2}^\dagger	3556.20 ± 0.09	3553	χ_{b2}^\dagger	9912.21 ± 0.26	9913
1^3P_1	χ_{c1}^\dagger	3510.66 ± 0.07	3502	χ_{b1}^\dagger	$9892.78 \pm 0.26 \pm 0.31$	9891
1^3P_0	χ_{c0}^\dagger	3414.75 ± 0.31	3429	χ_{b0}^\dagger	$9859.44 \pm 0.42 \pm 0.31$	9860
1^1P_1	h_c^\dagger	3525.41 ± 0.16	3524			9900
2^3P_2	$\chi_{c2}(2P)$	3927.2 ± 2.6	4125	$\chi_{b2}(2P)$	$10\,268.65 \pm 0.22 \pm 0.50$	10380
2^3P_1			4088	$\chi_{b1}(2P)$	$10\,255.46 \pm 0.22 \pm 0.50$	10364
2^3P_0			4043	$\chi_{b0}(2P)$	$10\,232.5 \pm 0.4 \pm 0.5$	10343
2^1P_1			4104			10370
3^3P_2			4615			10766
3^3P_1			4589			10754
3^3P_0			4561			10738
3^1P_1			4600			10759
1^3D_3			3878			10205
1^3D_2			3851	$\Upsilon(1D)$	$10\,163.7 \pm 1.4$	10195
1^3D_1	$\psi(3770)$	3772.92 ± 0.35	3821			10184
1^1D_2			3858			10198
2^3D_3			4386			10607
2^3D_2			4365			10598
2^3D_1	$\psi(4160)$	4153 ± 2.6	4344			10589
2^1D_2			4370			10600
3^3D_3			4846			10960
3^3D_2			4831			10952
3^3D_1			4817			10945
3^1D_2			4835			10954

Compared to Charmonium we obtain a better fit for Bottomonium. Our models seems to do well in explaining both $1P$ and $2P$ splittings.

We note that our model predicts only slightly higher value for $\Upsilon(3S)$ and $\Upsilon(4S)$ states.

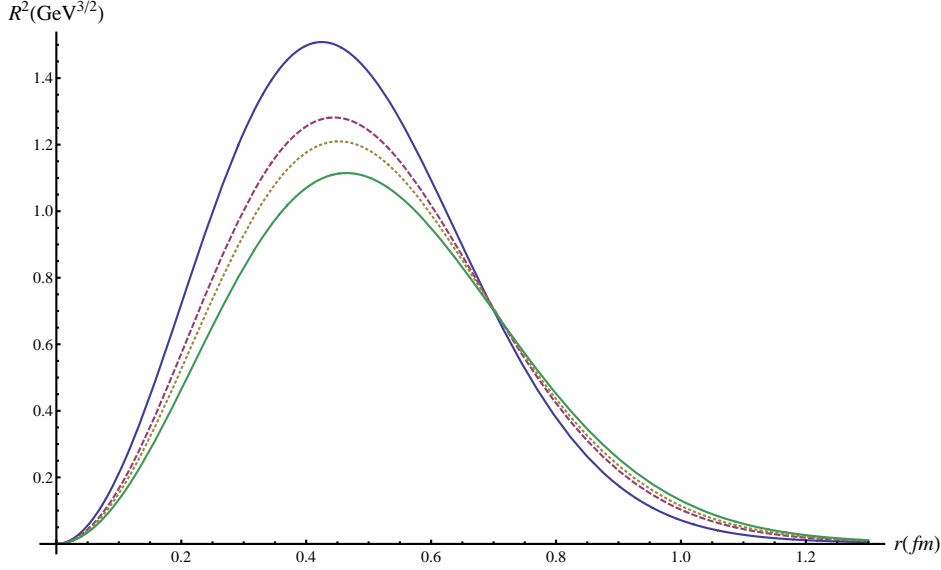


Figure 4.4: Squared radial wavefunctions for χ_0 (blue straight), χ_1 (red dashed), h_c (green dot-dashed) and χ_2 (black-thick)

The success of our model for Bottomonium may be attributed to b quarks high mass, which suits our non-relativistic approximation. Also we note that comparing the plots given for $1P$ Charmonium (Fig.3) and Bottomonium (Fig.6) states, Charmonium $1P$ states are split heavily by the spin-orbit coupling and the tensor force, while Bottomonium states show same regularity. This can be attributed to the fact that spin-orbit and tensor forces are proportional to the square of the inverse mass, $\left(\frac{1}{m_q}\right)$. Therefore it may be concluded that to model Charmonium better we need to consider a relativistic model or include higher order relativistic corrections.

4.3 E1 and M1 Radiative Transitions

To calculate the partial widths of the E1 radiative transitions we use[19],

$$\Gamma_{E1} \left(n^{2S+1} L_J \rightarrow n'^{2S'+1} L'_{J'} + \gamma \right) = \frac{4}{3} C_{fi} \delta_{SS'} e_q^2 \alpha \left| \langle R_f | r | R_i \rangle \right|^2 E_\gamma^3 \quad (4.3)$$

where, e_q is the quark charge, α is the fine-structure constant and E_γ is the final photon energy, given as $E_\gamma = (M_f - M_i)^2 / 2M_i$ in terms of the masses of the initial and final mesons. The matrix element C_{fi} is given as,

$$C_{fi} = \max(L, L')(2J' + 1) \begin{Bmatrix} L' & J' & S \\ J & L & 1 \end{Bmatrix} \quad (4.4)$$

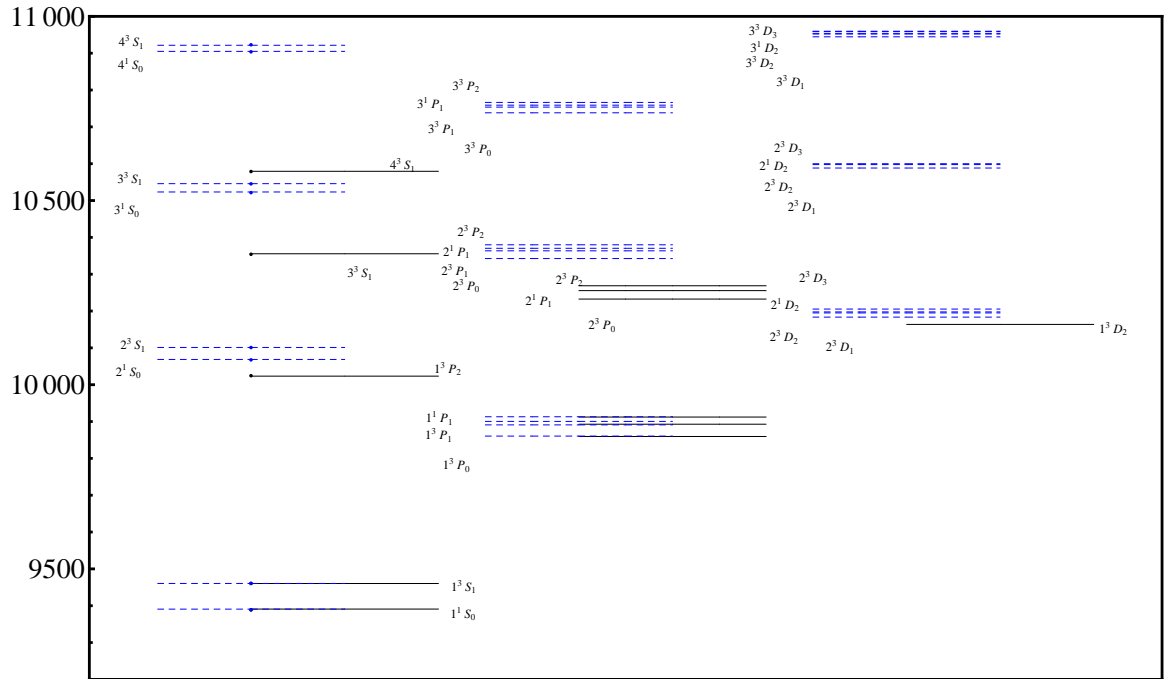


Figure 4.5: Bottomonium Spectrum Showing Experimental Measurements(Black) vs. Fitted Mass Values (Blue, dotted).

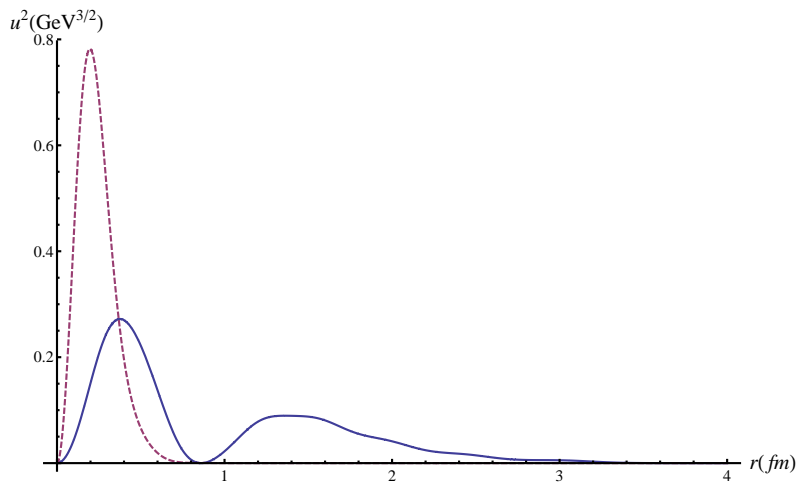


Figure 4.6: Squared reduced radial wavefunctions for η_b (blue straight) and $\Upsilon(1S)$ (red dashed)

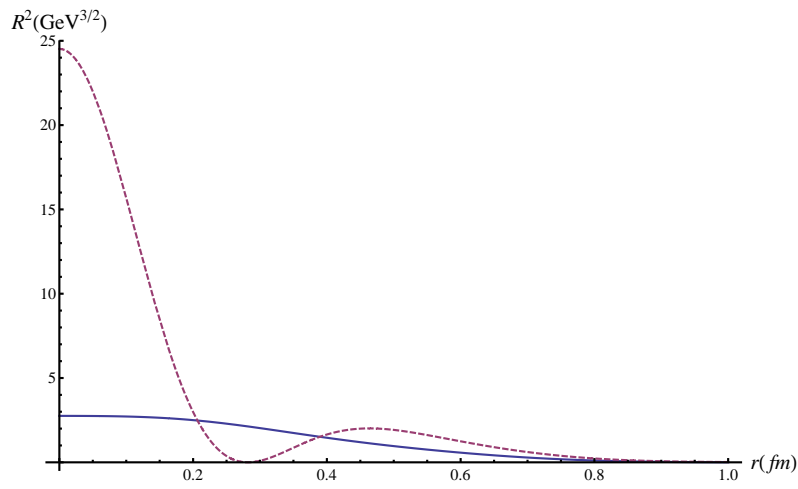


Figure 4.7: Squared radial wavefunctions for $\eta_b(2S)$ (blue straight) and $\Upsilon(2S)$ (red dashed)

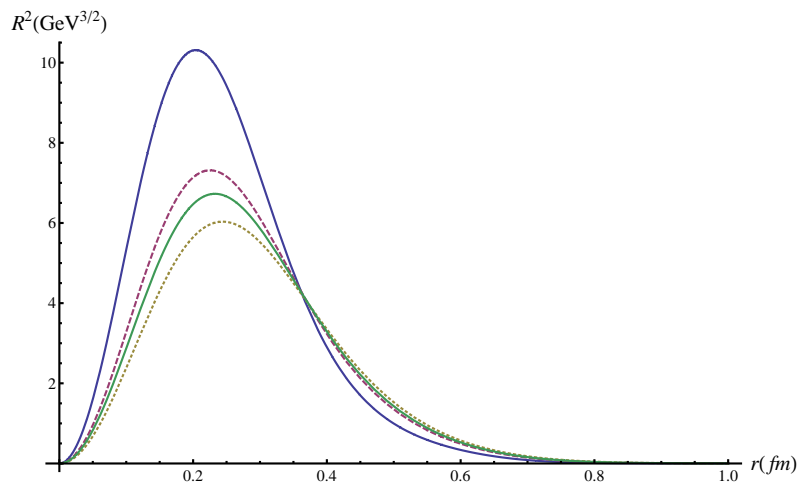


Figure 4.8: Squared radial wavefunctions for χ_{b0} (blue straight), χ_{b1} (red dashed), h_b (green dot-dashed) and χ_{b2} (black-thick)

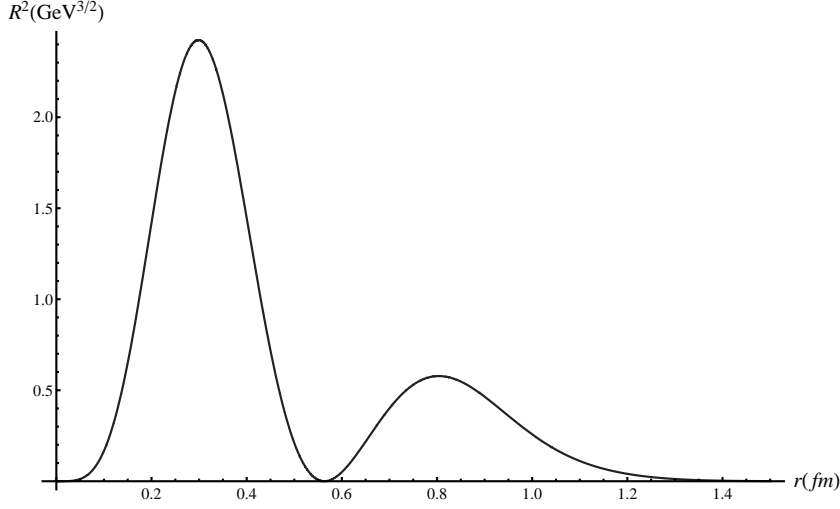


Figure 4.9: Squared radial wavefunctions for $Y(1D)$

To calculate the matrix elements, $|\langle R_f | r | R_i \rangle|$, where R represents the radial wavefunction of the meson, we use the reduced radial wave functions calculated previously, therefore,

$$|\langle R_f | r | R_i \rangle| = \int_0^\infty r dr u_{q\bar{q};k_f,j_f,l_f,s_f} u_{q\bar{q};k_i,j_i,l_i,s_i} \quad (4.5)$$

For M1 transitions we use[19],

$$\Gamma_{M1} (n^{2S+1} L_J \rightarrow n'^{2S'+1} L'_{J'} + \gamma) = \frac{4}{3} \frac{2J'+1}{2L+1} \delta_{S,S'+1} \delta_{LL'} \frac{e_q^2}{m_q^2} \alpha |\langle R_f | R_i \rangle|^2 E_\gamma^3 \quad (4.6)$$

The results of the calculations are given in the Tables [4.2-4.9]. For the masses of the initial and final states we use the experimental values only if experimental value is available for both the initial and the final state, otherwise we use the calculated mass values given in the preceding section.

Comparing with the experimental data we conclude that our calculations are at the same order with the experimental results, therefore verifying that M1 rates to be highly suppressed. As mentioned in the preceding section, a relativistic model may give better results. Also we note that we observed a high dependence of the matrix elements on the parameters, further study is required to refine the method.

Table 4.2: Partial widths of, $c\bar{c}$ E1 radiative transitions from S states.

	Initial state	Final state	$E_\gamma(MeV)$	$ \langle f r i \rangle $	$\Gamma_{th.}(keV)$	$\Gamma_{exp}(keV)$
2S→1P	$\psi'(2^3S_1)$	$\chi_2(1^3P_2)$	127.6	2.6899	36.59	26.6 ± 1.9
		$\chi_1(1^3P_1)$	171.3	2.374	40.80	27.9 ± 2.0
		$\chi_0(1^3P_0)$	197.8	1.831	28.77	29.4 ± 1.8
	$\eta'_c(2^1S_0)$	$h_c(1^1P_1)$	109.9	2.991	51.34	
3S→2P	$\psi(3^3S_1)$	$\chi_2(2^3P_2)$	110.3	4.052	52.89	
		$\chi_1(2^3P_1)$	264.0	3.540	332.5	
		$\chi_0(2^3P_0)$	335.0	2.768	138.5	
	$\eta_c(3^1S_0)$	$h_c(2^1P_1)$	154.5	2.557	104.4	
3S→1P	$\psi'(3^3S_1)$	$\chi_2(1^3P_2)$	453.9	0.1337	4.020	<0.015
		$\chi_1(1^3P_1)$	493.7	0.2345	9.548	<0.0095
		$\chi_0(1^3P_0)$	576.0	0.3264	9.786	
	$\eta'_c(3^1S_0)$	$h_c(1^1P_1)$	480.9	0.09167	4.043	
4S→3P	$\psi(4^3S_1)$	$\chi_2(3^3P_2)$	198.3	5.155	497.7	
		$\chi_1(3^3P_1)$	241.3	4.486	407.6	
		$\chi_0(3^3P_0)$	300.5	3.558	165.1	
	$\eta_c(4^1S_0)$	$h_c(3^1P_1)$	222.7	5.630	409.4	
4S→2P	$\psi(4^3S_1)$	$\chi_2(2^3P_2)$	219.7	0.2059	1.080	
		$\chi_1(2^3P_1)$	669.4	0.3569	55.10	
		$\chi_0(2^3P_0)$	733.7	0.4725	42.38	
	$\eta_c(4^1S_0)$	$h_c(2^1P_1)$	579.5	0.09584	7.733	
4S→1P	$\psi(4^3S_1)$	$\chi_2(1^3P_2)$	775.3	0.05045	2.850	
		$\chi_1(1^3P_1)$	811.7	0.09822	7.439	
		$\chi_0(1^3P_0)$	886.9	0.1541	7.959	
	$\eta_c(4^1S_0)$	$h_c(1^1P_1)$	1034	0.03386	5.484	

Table 4.3: Partial widths of, $b\bar{b}$ E1 radiative transitions from S states.

	Initial state	Final state	$E_\gamma(MeV)$	$\langle f r i \rangle$	$\Gamma_{th.}(keV)$	$\Gamma_{exp}(keV)$
2S→1P	$\Upsilon(2^3S_1)$	$\chi_{b2}(1^3P_2)$	110.4	-1.536	1.908	2.72 ± 0.32
		$\chi_{b1}(1^3P_1)$	171.3	-1.460	3.860	2.62 ± 0.33
		$\chi_{b0}(1^3P_0)$	162.7	-1.359	0.1650	1.44 ± 0.252
	$\eta_b(2^1S_0)$	$h_b(1^1P_1)$	167.6	0.1899	0.1835	
3S→2P	$\Upsilon(3^3S_1)$	$\chi_{b2}(2^3P_2)$	85.64	-1.231	0.5715	2.66 ± 0.57
		$\chi_{b1}(2^3P_1)$	99.06	-1.221	0.5228	2.56 ± 0.48
		$\chi_{b0}(2^3P_0)$	121.8	1.210	0.3178	1.20 ± 0.23
	$\eta_b(3^1S_0)$	$h_b(2^1P_1)$	151.9	-0.927	3.253	
3S→1P	$\Upsilon(3^3S_1)$	$\chi_{b2}(1^3P_2)$	432.8	-0.04149	0.0838	<0.37
		$\chi_{b1}(1^3P_1)$	451.9	0.06956	0.1610	<0.35
		$\chi_{b0}(1^3P_0)$	483.9	0.1050	0.1500	0.061 ± 0.028
	$\eta_b(3^1S_0)$	$h_b(1^1P_1)$	480.9	0.01269	0.03845	
4S→3P	$\Upsilon(4^3S_1)$	$\chi_{b2}(3^3P_2)$	154.9	3.011	20.23	
		$\chi_{b1}(3^3P_1)$	166.7	2.895	14.00	
		$\chi_{b0}(3^3P_0)$	182.5	2.754	5.533	
	$\eta_b(4^1S_0)$	$h_b(3^1P_1)$	145.0	3.098	31.68	
4S→2P	$\Upsilon(4^3S_1)$	$\chi_{b2}(2^3P_2)$	306.186	0.08973	0.1389	
		$\chi_{b1}(2^3P_1)$	319.0	0.1345	0.2117	
		$\chi_{b0}(2^3P_0)$	341.2	-0.1832	0.1603	
	$\eta_b(4^1S_0)$	$h_b(2^1P_1)$	521.9	1.489	340.8	
4S→1P	$\Upsilon(4^3S_1)$	$\chi_{b2}(1^3P_2)$	646.2	0.01987	0.06403	
		$\chi_{b1}(1^3P_1)$	664.3	0.03492	0.1289	
		$\chi_{b0}(1^3P_0)$	695.5	0.05386	0.1173	
	$\eta_b(4^1S_0)$	$h_b(1^1P_1)$	958.7	-0.8378	668.8	

Table 4.4: Partial widths of, $c\bar{c}$ E1 radiative transitions from P states.

	Initial state	Final state	$E_\gamma(MeV)$	$ \langle f r i \rangle $	$\Gamma_{th.}(keV)$	$\Gamma_{exp}(keV)$
1P→1S	$\chi_2(1^3P_2)$	$J/\psi(1^3S_1)$	429.6	2.514	722.8	384±37
	$\chi_1(1^3P_1)$		389.4	2.536	547.3	296±30
	$\chi_0(1^3P_0)$		303.0	2.519	254.7	122±15
	$h_c(1^1P_1)$	$\eta_c(1^1S_0)$	503.0	0.8986	148.2	387±281±200
2P→2S	$\chi_2(2^3P_2)$	$\psi'(2^3S_1)$	115	3.843	32.52	
	$\chi_1(2^3P_1)$		248	4.076	363.1	
	$\chi_0(2^3P_0)$		175	4.326	144.7	
	$h_c(3^1P_1)$	$\eta'_c(2^1S_0)$	373	1.271	120.8	
2P→1S	$\chi_2(2^3P_2)$	$\psi'(1^3S_1)$	739.6	0.3132	57.24	
	$\chi_1(2^3P_1)$		850.7	0.1166	12.07	
	$\chi_0(2^3P_0)$		789.8	0.2350	39.24	
	$h_c(2^1P_1)$	$\eta'_c(1^1S_0)$	1012	0.4567	311.36	
2P→1D	$\chi_2(2^3P_2)$	$\psi_3(1^3D_3)$	53.49	2.725	2.753	
		$\psi_2(1^3D_2)$	83.02	2.506	1.554	
		$\psi(1^3D_1)$	117.38	2.250	0.236	
	$\chi_1(2^3P_1)$	$\psi_2(1^3D_2)$	216.5	2.568	48.21	
		$\psi(1^3D_1)$	249.7	2.815	266.7	
	$\chi_0(2^3P_0)$	$\psi(1^3D_1)$	114.3	3.021	39.33	
	$h_c(2^1P_1)$	$\eta_{2c}(1^1D_2)$	528.4	0.5996	12.54	
3P→3S	$\chi_2(3^3P_2)$	$\psi'(1^3S_1)$	242.3	4.991	510.9	
	$\chi_1(3^3P_1)$		199.3	5.380	330.5	
	$\chi_0(3^3P_0)$		138.9	5.785	129.2	
	$h_c(3^1P_1)$	$\eta'_c(1^1S_0)$	305.7	4.090	689.0	
3P→2S	$\chi_2(3^3P_2)$	$\psi'(1^3S_1)$	711.3	0.3606	67.49	
	$\chi_1(3^3P_1)$		673.0	0.09766	4.192	
	$\chi_0(3^3P_0)$		619.2	0.3628	45.06	
	$h_c(3^1P_1)$	$\eta'_c(1^1S_0)$	783.6	0.5514	210.9	
3P→1S	$\chi_2(3^3P_2)$	$\psi'(1^3S_1)$	1246	0.1244	43.18	
	$\chi_1(3^3P_1)$		1213	0.01131	0.3290	
	$\chi_0(3^3P_0)$		1167	0.1469	49.39	
	$h_c(3^1P_1)$	$\eta'_c(1^1S_0)$	1356	0.2321	193.6	

Table 4.5: Partial widths of, $c\bar{c}$ E1 radiative transitions from P states (continued).

	Initial state	Final state	$E_\gamma(MeV)$	$ \langle f r i \rangle $	$\Gamma_{th.}(keV)$	$\Gamma_{exp}(keV)$
3P→2D	$\chi_2(3^3P_2)$	$\psi_3(2^3D_3)$	213.0	4.014	377.1	
		$\psi_2(2^3D_2)$	239.1	2.474	36.20	
		$\psi(2^3D_1)$	268.9	3.299	6.101	
	$\chi_1(3^3P_1)$	$\psi_2(2^3D_2)$	196.1	2.474	19.97	
		$\psi(2^3D_1)$	226.2	3.299	3.632	
	$\chi_0(3^3P_0)$	$\psi(2^3D_1)$	166.1	3.299	1.438	
	$h_c(3^1P_1)$	$\eta_{2c}(2^1D_2)$	207.8	4.755	585.0	
3P→1D	$\chi_2(3^3P_2)$	$\psi_3(2^3D_3)$	658.5	1.426	1406	
		$\psi_2(2^3D_2)$	683.8	0.2001	5.567	
		$\psi(2^3D_1)$	713.2	0.2456	0.6309	
	$\chi_1(3^3P_1)$	$\psi_2(2^3D_2)$	645.2	0.1718	5.714	
		$\psi(2^3D_1)$	674.9	-2.815	5270	
	$\chi_0(3^3P_0)$	$\psi(2^3D_1)$	565.1	1.603×10^{-3}	1.338×10^{-3}	
	$h_c(3^1P_1)$	$\eta_{2c}(2^1D_2)$	655.2	1.322	1418	

Table 4.6: Partial widths of, $b\bar{b}$ E1 radiative transitions from P states.

	Initial state	Final state	$E_\gamma(MeV)$	$\langle f r i \rangle$	$\Gamma_{th.}(keV)$	$\Gamma_{exp}(keV)$
1P→1S	$\chi_2(1^3P_2)$	$J/\psi(1^3S_1)$	441.6	1.223	46.43	
	$\chi_1(1^3P_1)$		423.0	1.233	41.45	
	$\chi_0(1^3P_0)$		391.1	1.242	33.25	
	$h_c(1^1P_1)$	$\eta_c(1^1S_0)$	430.2	0.03314	0.03153	
2P→2S	$\chi_2(2^3P_2)$	$\psi'(2^3S_1)$	242.5	1.260	8.153	
	$\chi_1(3^3P_1)$		229.6	1.241	6.782	
	$\chi_0(3^3P_0)$		207.1	-1.219	4.755	
	$h_c(3^1P_1)$	$\eta'_c(2^1S_0)$	296.6	-0.3909	1.438	
2P→1S	$\chi_2(2^3P_2)$	$\psi'(1^3S_1)$	776.5	0.2132	7.670	
	$\chi_1(2^3P_1)$		764.3	0.1755	19.84	
	$\chi_0(2^3P_0)$		743.1	-0.1236	4.960	
	$h_c(2^1P_1)$	$\eta'_c(1^1S_0)$	932.8	0.06485	1.231	
2P→1D	$\chi_2(2^3P_2)$	$\psi_3(1^3D_3)$	173.5	0.3933	0.4895	
		$\psi_2(1^3D_2)$	66.28	0.38	0.003480	
		$\psi(1^3D_1)$	194.2	-0.1294	0.8835×10^{-3}	
	$\chi_1(2^3P_1)$	$\psi_2(1^3D_2)$	157.8	-0.1246	0.01099	
		$\psi(1^3D_1)$	91.35	-1.6216	1.084	
	$\chi_0(2^3P_0)$	$\psi(1^3D_1)$	157.8	0.1187	0.03993	
	$h_c(2^1P_1)$	$\eta_{2c}(1^1D_2)$	170.6	0.4167	0.6213	
3P→3S	$\chi_2(3^3P_2)$	$\psi'(1^3S_1)$	217.8	-1.161	20.07	
	$\chi_1(3^3P_1)$		206.0	1.304	21.44	
	$\chi_0(3^3P_0)$		190.3	1.313	17.13	
	$h_c(3^1P_1)$	$\eta'_c(1^1S_0)$	233.4	1.364	34.13	
3P→2S	$\chi_2(3^3P_2)$	$\psi'(2^3S_1)$	644.5	0.2518	5.018	
	$\chi_1(3^3P_1)$		633.2	0.6832	42.70	
	$\chi_0(3^3P_0)$		618.1	0.1455	1.801	
	$h_c(3^1P_1)$	$\eta'_c(2^1S_0)$	667.9	0.2922	9.165	
3P→1S	$\chi_2(3^3P_2)$	$\psi'(1^3S_1)$	1227	0.09697	6.258	
	$\chi_1(3^3P_1)$		1216	0.07465	3.613	
	$\chi_0(3^3P_0)$		1202	0.04686	1.375	
	$h_c(3^1P_1)$	$\eta'_c(1^1S_0)$	1281	-0.1242	11.68	

Table 4.7: Partial widths of, $b\bar{b}$ E1 radiative transitions from P states (continued).

	Initial state	Final state	$E_\gamma(MeV)$	$\langle f r i \rangle$	$\Gamma_{th.}(keV)$	$\Gamma_{exp}(keV)$
3P→2D	$\chi_2(3^3P_2)$	$\psi_3(2^3D_3)$	157.83	-0.7177	4.905	
		$\psi_2(2^3D_2)$	166.7	0.7097	1.009	
		$\psi(2^3D_1)$	175.6	0.7014	0.07674	
	$\chi_1(3^3P_1)$	$\psi_2(2^3D_2)$	154.9	0.7097	0.8092	
		$\psi(2^3D_1)$	163.7	0.7014	0.06228	
	$\chi_0(3^3P_0)$	$\psi(2^3D_1)$	148.0	0.7014	0.04596	
	$h_c(3^1P_1)$	$\eta_{2c}(2^1D_2)$	157.8	0.9487	10.20	
3P→1D	$\chi_2(3^3P_2)$	$\psi_3(2^3D_3)$	546.4	0.05374	1.141	
		$\psi_2(2^3D_2)$	555.9	-0.07087	0.3731	
		$\psi(2^3D_1)$	566.3	0.3126	0.5116	
	$\chi_1(3^3P_1)$	$\psi_2(2^3D_2)$	645.2	-0.1718	5.714	
		$\psi(2^3D_1)$	554.9	-0.1611	9.589	
	$\chi_0(3^3P_0)$	$\psi(2^3D_1)$	539.7	0.02063	0.1930	
	$h_c(3^1P_1)$	$\eta_{2c}(2^1D_2)$	546.4	-0.05250	1.297	

Table 4.8: Partial widths of, $c\bar{c}$ M1 radiative transitions.

Multiplet	Initial state	Final state	$E_\gamma(MeV)$	$ \langle f i \rangle $	$\Gamma_{th.}(keV)$	$\Gamma_{exp}(keV)$
1S	$J/\Psi(1^3S_1)$	$\eta_c(1^1S_0)$	114.4	0.9677	3.736	1.6 ± 0.4
2S	$\psi'(2^3S_1)$	$\eta'_c(2^1S_0)$	48.76	0.9523	0.2801	<0.2
		$\eta_c(1^1S_0)$	638.2	0.1116	8.623	1.0 ± 0.2
	$\eta'_c(2^1S_0)$	$J/\Psi(1^3S_1)$	500.0	0.1289	16.60	
3S	$\psi(3^3S_1)$	$\eta_c(3^1S_0)$	92.15	0.2507	0.1310	
		$\eta'_c(2^1S_0)$	382.0	0.1613	3.862	
		$\eta_c(1^1S_0)$	920.0	0.1071	23.79	
	$\eta_c(3^1S_0)$	$\psi'(2^3S_1)$	337.5	0.2135	14.00	
		$J/\Psi(1^3S_1)$	832.2	0.09521	41.75	
1P	$h_c(1^1P_1)$	$\chi_{c1}(1^3P_1)$	14.72	0.9991	8.477×10^{-3}	
		$\chi_{c0}(1^3P_0)$	108.9	0.9804	1.103	
	$\chi_{c2}(1^3P_2)$	$h_c(1^1P_1)$	30.66	0.9985	0.0765	
2P	$h_c(2^1P_1)$	$\chi_{c1}(2^3P_1)$	21.90	0.2875	2.309×10^{-3}	
		$\chi_{c0}(2^3P_0)$	97.24	0.2756	0.06200	
		$\chi_{c2}(1^3P_2)$	500.7	0.04576	1.167	
		$\chi_{c1}(1^3P_1)$	550.9	0.04534	0.9156	
		$\chi_{c0}(1^3P_0)$	636.9	0.07005	1.125	
	$\chi_{c2}(2^3P_2)$	$h_c(2^1P_1)$	27.50	0.2957	4.844×10^{-3}	
		$h_c(1^1P_1)$	552.4	0.04389	0.8648	
	$\chi_{c1}(2^3P_1)$	$h_c(1^1P_1)$	509.3	0.03689	0.4785	
$\chi_{c0}(2^3P_0)$	$h_c(1^1P_1)$	441.8	0.04493	0.4635		
1P	$\psi(1^1D_2)$	$\psi(1^3D_2)$	6.994	0.9999	0.9109×10^{-3}	
		$\psi(1^3D_1)$	36.82	0.9493	0.1198	
	$\psi(1^3D_3)$	$\psi(1^1D_2)$	19.95	0.9993	0.02111	
2D	$\psi(2^1D_2)$	$\psi(2^3D_2)$	4.997	0.9998	0.3322×10^{-3}	
		$\psi(2^3D_1)$	25.92	0.9944	0.02752	
		$\psi(1^3D_3)$	464.3	0.03212	0.3850	
		$\psi(1^3D_2)$	488.2	0.009423	0.02752	
		$\psi(1^3D_1)$	514.5	0.05644	0.6932	
	$\psi(2^3D_3)$	$\psi(2^1D_2)$	27.50	0.9981	0.05520	
		$\psi(1^1D_2)$	552.4	0.04389	0.8648	
	$\psi(2^3D_2)$	$\psi(1^1D_2)$	509.3	0.03688	0.4785	
$\psi(2^3D_1)$	$\psi(1^1D_2)$	441.8	0.04493	0.4635		

Table 4.9: Partial widths of, $b\bar{b}$ M1 radiative transitions.

Multiplet	Initial state	Final state	$E_\gamma(MeV)$	$ \langle f i \rangle $	$\Gamma_{th.}(keV)$	$\Gamma_{exp}(keV)$
1S	$\Upsilon(1^3S_1)$	$\eta_b(1^1S_0)$	69.14	0.07639	0.09733×10^{-3}	
2S	$\Upsilon(2^3S_1)$	$\eta_b(2^1S_0)$	31.95	0.9978	1.638×10^{-3}	0.013±0.006
		$\eta_b(1^1S_0)$	612.2	0.07053	0.05755	
	$\eta_b(2^1S_0)$	$\Upsilon(1^3S_1)$	655.2	0.07383	0.2320	
3S	$\Upsilon(3^3S_1)$	$\eta_b(3^1S_0)$	92.15	0.2507	0.03275	<0.013 0.010±0.002
		$\eta_b(2^1S_0)$	22.98	0.3173	0.06160×10^{-3}	
		$\eta_b(1^1S_0)$	466.21	0.03698	0.006988	
	$\eta_b(3^1S_0)$	$\Upsilon(2^3S_1)$	413.5	0.3164	1.071	
		$\Upsilon(1^3S_1)$	1009	0.03443	0.1844	
1P	$h_b(1^1P_1)$	$\chi_{b1}(1^3P_1)$	8.996	0.03677	0.0497×10^{-6}	
		$\chi_{b0}(1^3P_0)$	39.92	0.03449	1.272×10^{-6}	
	$\chi_{b2}(1^3P_2)$	$h_b(1^1P_1)$	21.98	0.03856	0.7960×10^{-6}	
2P	$h_b(2^1P_1)$	$\chi_{b1}(2^3P_1)$	5.998	0.1528	0.2540×10^{-6}	
		$\chi_{b0}(2^3P_0)$	26.97	0.1627	0.008725×10^{-3}	
		$\chi_{b2}(1^3P_2)$	446.9	0.08379	0.0527	
		$\chi_{b1}(1^3P_1)$	467.9	0.08008	0.03315	
		$\chi_{b0}(1^3P_0)$	497.5	0.07529	0.01173	
	$\chi_{b2}(2^3P_2)$	$h_b(2^1P_1)$	5.998	0.1684	0.3085×10^{-6}	
		$h_b(1^1P_1)$	26.97	0.08251	0.006732×10^{-3}	
	$\chi_{b1}(2^3P_1)$	$h_b(1^1P_1)$	453.6	0.08103	0.0309	
		$\chi_{b0}(2^3P_0)$	$h_b(1^1P_1)$	433.5	0.07926	
1D	$\Upsilon(1^1D_2)$	$\Upsilon(1^3D_2)$	3.000	1.000	1.361×10^{-6}	
		$\Upsilon(1^3D_1)$	36.82	0.9493	0.02995	
	$\Upsilon(1^3D_3)$	$\Upsilon(1^1D_2)$	6.998	1.000	0.01728×10^{-6}	
2D	$\Upsilon(2^1D_2)$	$\Upsilon(2^3D_2)$	2.000	0.09863	0.03925×10^{-9}	
		$\Upsilon(2^3D_1)$	25.92	0.9944	0.006880	
		$\Upsilon(1^3D_3)$	387.6	0.01357	0.7575×10^{-3}	
		$\Upsilon(1^3D_2)$	397.3	0.004793	0.7265×10^{-3}	
		$\Upsilon(1^3D_1)$	407.8	0.04187	0.003598	
	$\Upsilon(2^3D_3)$	$\Upsilon(2^1D_2)$	7.000	0.1684	0.490×10^{-6}	
		$\Upsilon(1^1D_2)$	401.1	0.08251	0.02216	
	$\Upsilon(2^3D_2)$	$\Upsilon(1^1D_2)$	392.5	0.08104	0.02000	
	$\Upsilon(2^3D_1)$	$\Upsilon(1^1D_2)$	383.8	0.07926	0.01791	

CHAPTER 5

CONCLUSION

In this work we investigate the Charmonium and Bottomonium spectra and radiative decays using the basic assumptions of the quark model.

We adopted the hypothesis that spin dependent potentials are attributable to the short distance part of the potential. For the short distance part, assuming that the perturbative approach works, we have derived the Coulomb interaction and a relativistic correction to the first order, the Breit Interaction. By making a non-relativistic reduction via Foldy-Wouthuysen transformation we extracted spin-dependent potential from one gluon exchange and explained the physical meaning of the various parts of the potential.

Furthermore we present our method of using 3D harmonic oscillator solutions to diagonalize the derived Hamiltonian therefore obtaining the masses and wavefunctions of $c\bar{c}$ and $b\bar{b}$ mesons. Using these wavefunctions we also calculate the partial widths of the radiative E1 and M1 decays.

Finally we present the results of our analysis for the spectrum of Charmonium and Bottomonium and the fitted values of the parameters, m_c , m_b , σ , α_s . We also give plots of the radial wavefunctions for some Bottomonium and Charmonium states. For the $b\bar{b}$ the predicted mass values agree well with the experiments whereas for $c\bar{c}$, our model fails to predict the spectrum precisely. By comparing with the experimental and lattice results we comment on the shortcomings of our method.

All in all we believe that, this study was beneficial in investigating the fundamental assumptions of the Quark Model and setting up a crude model for the Charmonium and Bottomonium systems that can explain the fundamental properties of the spectrum. For a more detailed

analysis, a relativized approach together with a procedure to take $B\bar{B}$ and $D\bar{D}$ thresholds into account must be followed. In such a scheme consideration of light quarks would be possible.

REFERENCES

- [1] WA Barker and FN Glover, *Reduction of Relativistic Two-Particle Wave Equations to Approximate Forms. III*, Physical Review **99** (1955), no. 1, 317.
- [2] T. Barnes, *The XYZs of Charmonium at BES*, International Journal of Modern Physics A **21** (2006), no. 27, 5583–5591.
- [3] T. Barnes, S. Godfrey, and ES Swanson, *Higher charmonia*, Physical Review D **72** (2005), no. 5, 054026.
- [4] GC Bhatt, H. Grotch, and X. Zhang, *Scalar confinement potential in charmonium*, Journal of Physics G: Nuclear and Particle Physics **17** (1991), 231.
- [5] JD Bjorken and SD Drell, *Relativistic quantum mechanics*, Wiley-VCH, 1964.
- [6] N. Brambilla, S. Eidelman, B. K. Heltsley, R. Vogt, G. T. Bodwin, E. Eichten, a. D. Frawley, a. B. Meyer, R. E. Mitchell, V. Papadimitriou, P. Petreczky, a. a. Petrov, P. Robbe, a. Vairo, a. Andronic, R. Arnaaldi, P. Artoisenet, G. Bali, a. Bertolin, D. Bettoni, J. Brodzicka, G. E. Bruno, a. Caldwell, J. Catmore, C.-H. Chang, K.-T. Chao, E. Chudakov, P. Cortese, P. Crochet, a. Drutskoy, U. Ellwanger, P. Faccioli, a. Gaba-reenÂ Mokhtar, X. GarciaÂ iÂ Tormo, C. Hanhart, F. a. Harris, D. M. Kaplan, S. R. Klein, H. Kowalski, J.-P. Lansberg, E. Levichev, V. Lombardo, C. Lourenço, F. Maltoni, a. Mocsy, R. Mussa, F. S. Navarra, M. Negrini, M. Nielsen, S. L. Olsen, P. Pakhlov, G. Pakhlova, K. Peters, a. D. Polosa, W. Qian, J.-W. Qiu, G. Rong, M. a. Sanchis-Lozano, E. Scomparin, P. Senger, F. Simon, S. Stracka, Y. Sumino, M. Voloshin, C. Weiss, H. K. Wöhri, and C.-Z. Yuan, *Heavy quarkonium: progress, puzzles, and opportunities*, The European Physical Journal C **71** (2011), no. 2, 1–178.
- [7] Nora Brambilla, *Current Topics in Heavy Quarkonium Physics*, (2011), 14.
- [8] Nora Brambilla, Antonio Vairo, and Thomas Rösch, *Effective field theory Lagrangians for baryons with two and three heavy quarks*, Physical Review D **72** (2005), no. 3, 1–17.
- [9] G. Breit, *The effect of retardation on the interaction of two electrons*, Physical Review **34** (1929), no. 4, 553.
- [10] V. Zeno Chraplyvy, *Reduction of Relativistic Two-Particle Wave Equations to Approximate Forms. I*, Physical Review **91** (1953), no. 2, 388–391.
- [11] Z.V. Chraplyvy, *Reduction of relativistic two-particle wave equations to approximate forms. ii*, Physical Review **92** (1953), no. 5, 1310.
- [12] ATLAS Collaboration, *Observation of a New b State in Radiative Transitions to (1S) and (2S) at ATLAS*, Physical Review Letters (2011), 1–17.
- [13] TP Das, *Relativistic quantum mechanics of electrons*, Harper & Row, 1973.

- [14] A. De Rujula, H. Georgi, and SL Glashow, *Hadron masses in a gauge theory*, Physical Review D **12** (1975), no. 1, 147.
- [15] M. De Sanctis, *A generalization of the Fermi-Breit equation to non-Coulombic spatial interactions*, The European Physical Journal A **41** (2009), no. 2, 169–178.
- [16] M. De Sanctis and P. Quintero, *Charmonium spectrum with a generalized Fermi-Breit equation*, The European Physical Journal A **46** (2010), no. 2, 213–221.
- [17] E. Eichten, K. Gottfried, T. Kinoshita, J Kogut, KD Lane, and T.M. Yan, *Spectrum of charmed quark-antiquark bound states*, Physical Review Letters **34** (1975), no. 6, 369–372.
- [18] E. Eichten, K. Gottfried, T. Kinoshita, KD Lane, and T.M. Yan, *Charmonium: the model*, Physical Review D **17** (1978), no. 11, 3090.
- [19] E. Eichten, K. Gottfried, T. Kinoshita, KD Lane, and TM Yan, *Charmonium: Comparison with experiment*, Physical Review D **21** (1980), no. 1, 203.
- [20] L.L. Foldy and S.A. Wouthuysen, *On the Dirac theory of spin 1/2 particles and its non-relativistic limit*, Physical Review **78** (1950), no. 1, 29.
- [21] S. Gasiorowicz and J.L. Rosner, *Hadron spectra and quarks*, American Journal of Physics **49** (1981), 954.
- [22] S. Godfrey and N. Isgur, *Mesons in a relativized quark model with chromodynamics*, Physical Review D **32** (1985), no. 1, 189.
- [23] OW Greenberg, *Resource Letter Q-1: Quarks*, American Journal of Physics (1982).
- [24] D Griffiths, *Introduction to Elementary Particles*, Wiley-VCH, 2004.
- [25] S.N. Gupta and S.F. Radford, *Quark-quark and quark-antiquark potentials*, Physical Review D **24** (1981), 2309–2323.
- [26] S.N. Gupta and SF Radford, *Remarks on quark-quark and quark-antiquark potentials*, Phys. Rev. D;(United States) **25** (1982), no. 12, 1829–1841.
- [27] S.N. Gupta, S.F. Radford, and W.W. Repko, *Quarkonium spectra and quantum chromodynamics*, Physical Review D **26** (1982), no. 11, 3305.
- [28] K. Hagiwara, K. Hikasa, K. Nakamura, M. Tanabashi, M. Aguilar-Benitez, C. Amsler, R.M. Barnett, PR Burchat, CD Carone, C. Caso, and Others, *Review of particle physics*, Physical Review D (2002).
- [29] JD Jackson, *Classical Electrodynamics*, third edit ed., John Wiley&Sons, Inc.
- [30] Taichi Kawanai and Shoichi Sasaki, *Charmonium potential from full lattice QCD*, **156** (2011), no. 7, 1–5.
- [31] Michael Klasen, Benno List, Stephanie Hansmann-Menzemer, and Rainer Mankel, *Summary of the Heavy Flavor Working Group*, Proceedings of the XV International Workshop on Deep-Inelastic Scattering and Related Subjectes, DIS 2007, July 2007, p. 17.
- [32] A Le Yaoquanc, LL Oliver, O Péne, and JC Raynal, *Hadron Transition in the Quark Model*, Gordon and Breach Science Publishers, 1988.

- [33] R. McClary and Nina Byers, *Relativistic effects in heavy-quarkonium spectroscopy*, Physical Review D **28** (1983), no. 7, 1692.
- [34] M. G. Olsson and K.J. Miller, *relativistic corrections in potential models*, Physical Review D **28** (1983), no. 3, 674–676.
- [35] Guillaume Plante and Adel F. Antippa, *Analytic solution of the Schrodinger equation for the Coulomb-plus-linear potential. I. The wave functions*, Journal of Mathematical Physics **46** (2005), no. 6, 062108.
- [36] J. Pumplin, W. Repko, and A. Sato, *Fine-structure corrections and electromagnetic decays of charmonium*, Physical Review Letters **35** (1975), no. 22, 1538–1540.
- [37] Quigg, C. and J.L. Rosner, *Quantum mechanics with applications to quarkonia*, Physics Reports **56**, no. 4, 167–235.
- [38] Stanley Radford and Wayne Repko, *Potential model calculations and predictions for heavy quarkonium*, Physical Review D **75** (2007), no. 7, 1–9.
- [39] Vladimir Sauli and Pedro Bicudo, *Excited charmonium states from Bethe-Salpeter equation*, Arxiv preprint arXiv:1112.5540 (2011).
- [40] H.J. Schnitzer, *p States of Charmonium and the Forces that Confine Quarks*, Physical Review Letters **35** (1975), no. 22, 1540–1543.
- [41] Y Sumino, *QCD potential as a Coulomb plus linear potential*, Physics Letters B **571** (2003), no. 3-4, 173–183.
- [42] Eric S. Swanson, *The new heavy mesons: A status report*, Physics Reports **429** (2006), no. 5, 243–305.
- [43] JG Wills, DB Lichtenberg, and JT Kiehl, *Meson spectrum in the quark model with a phenomenological potential*, Physical Review D **15** (1977), no. 11, 3358.

APPENDIX A

FOLDY-WOUTHUYSEN TRANSFORMATION

We start with a Dirac Hamiltonian for two particles with an arbitrary potential, V ,

$$H = \alpha^I \cdot \mathbf{p}^I + \alpha^{II} \cdot \mathbf{p}^{II} + \beta^I m_I + \beta^{II} m_{II} + V \quad (\text{A.1})$$

The Dirac matrices are 16×16 matrices, α^I and β^I operate on the spinor space of the first particle and α^{II} and β^{II} operate on those of the second particle, with elements given as,

$$(\alpha^I)_{jk,JK} = (\alpha^I)_{jk}(\delta)_{JK}, \quad (\beta^I)_{jk,JK} = (\beta^I)_{jk}(\delta)_{JK} \quad (\text{A.2})$$

$$(\alpha^{II})_{jk,JK} = (\delta)_{jk}(\alpha^{II})_{JK}, \quad (\beta^{II})_{jk,JK} = (\delta)_{jk}(\beta^{II})_{JK} \quad (\text{A.3})$$

Therefore the commutation relations are of the form,

$$(\alpha_n^{I(II)})^2 = (\beta_n^{I(II)})^2 = I_{16 \times 16} \quad (\text{A.4})$$

$$[(\alpha^I)_{jk,JK}, (\alpha^I)_{j'k',J'K'}]_+ = 2(\delta)_{kk'}(\delta)_{JJ'}(\delta)_{jj'}(\delta)_{KK'} \quad (\text{A.5})$$

Note that the operator $\alpha^{I(II)} \cdot \mathbf{p}^{I(II)}$ mixes states with negative and positive energy of the 1st(2nd), which is the result of the relativistic nature of the Dirac equation. In order to obtain a non-relativistic equation we need to remove this mixing. We identify such operators by considering their commutation with β^I and β^{II} . We label the operators as $\mathcal{E}\mathcal{E}$ (even-even) if they commute with β^I and β^{II} , $\mathcal{O}\mathcal{O}$ if they anti-commute with both β^I and β^{II} , and $\mathcal{E}\mathcal{O}(\mathcal{O}\mathcal{E})$ if they commute with $\beta^I(\beta^{II})$ and anti-commute with $\beta^{II}(\beta^I)$, i.e.,

$$[\mathcal{O}\mathcal{O}, \beta^I]_+ = [\mathcal{O}\mathcal{O}, \beta^{II}]_+ = 0 \quad (\text{A.6})$$

$$[\mathcal{E}\mathcal{E}, \beta^I] = [\mathcal{E}\mathcal{E}, \beta^{II}] = 0 \quad (\text{A.7})$$

$$[\mathcal{E}\mathcal{O}, \beta^{II}]_+ = [\mathcal{O}\mathcal{E}, \beta^I]_+ = 0 \quad (\text{A.8})$$

$$[\mathcal{E}\mathcal{O}, \beta^I] = [\mathcal{O}\mathcal{E}, \beta^{II}] = 0 \quad (\text{A.9})$$

Note that $\mathcal{E}\mathcal{E}$ operators do not mix negative and positive energy solutions of the neither 1st and 2nd particle whereas $\mathcal{O}\mathcal{O}$ mix both and $\mathcal{O}\mathcal{E}(\mathcal{E}\mathcal{O})$ mix only the negative and positive energy solutions of the 1st(2nd) particles.

The idea behind the Foldy-Wouthuysen transformation is to make a unitary transformation,

$$\Psi' = e^{iS}\Psi \quad (\text{A.10})$$

so that in the transformed Hamiltonian,

$$\frac{\partial}{\partial t}\Psi' = \frac{\partial}{\partial t}(e^{iS}\Psi) = e^{iS}\frac{\partial}{\partial t}\Psi = e^{iS}H\Psi = e^{iS}He^{-iS}e^{iS}\Psi = H'\Psi' \quad (\text{A.11})$$

$$H' = e^{iS}He^{-iS} \quad (\text{A.12})$$

the operators that result in mixing only contributes to the in the order $1/m^4$. Determination of the operator S in the case of one particle is very easy: First one expresses the transformed Hamiltonian as series expansion

$$H' = H + i[S, H] - \frac{1}{2!}[S, [S, H]] + \dots \quad (\text{A.13})$$

then requires the transformed Hamiltonian not to include the operators that mix negative and positive energy solutions at the first order. Therefore for a general case of Hamiltonian for one particle,

$$H = \mathcal{E} + \mathcal{O} + \beta m \quad (\text{A.14})$$

one chooses $S = -i\beta\mathcal{O}/m$ so that the transformed Hamiltonian includes the odd operator only at second order ($1/m^2$). For the case of two particles

$$H = \mathcal{E}\mathcal{E} + \mathcal{O}\mathcal{E} + \mathcal{E}\mathcal{O} + \mathcal{O}\mathcal{O} + \beta^I m_I + \beta^{II} m_{II} \quad (\text{A.15})$$

the transformation is given as[11],

$$\begin{aligned} H = & \beta^I m_I + \beta^{II} m_{II} + (\mathcal{E}\mathcal{E}) + \frac{\beta^I}{2m_I}(\mathcal{O}\mathcal{E})^2 + \frac{\beta^{II}}{2m_{II}}(\mathcal{E}\mathcal{O})^2 - \frac{\beta^I}{8m_I^3}(\mathcal{O}\mathcal{E})^2 - \frac{\beta^{II}}{8m_{II}^3}(\mathcal{E}\mathcal{O})^2 \\ & + \frac{1}{8m_I^2} [[\mathcal{O}\mathcal{E}, \mathcal{E}\mathcal{E}], \mathcal{O}\mathcal{E}] + \frac{1}{8m_I^2} [[\mathcal{E}\mathcal{O}, \mathcal{E}\mathcal{E}], \mathcal{O}\mathcal{E}] + \frac{\beta^I \beta^{II}}{4m_I - m_{II}} [[\mathcal{O}\mathcal{E}, \mathcal{O}\mathcal{O}]_+, \mathcal{O}\mathcal{E}]_+ \end{aligned} \quad (\text{A.16})$$

for particles with different mass, $m_I \neq m_{II}$. But for the case of equal masses obtaining S is a formidable task and the resulting tedious formula can be found at [11]. At first sight one might think that the formula given above can not be used for our case where the Hamiltonian is given by,

$$H_B = H_I + H_{II} + U_B(\mathbf{r}) \quad (\text{A.17})$$

where, in CM coordinates,

$$H_I = \alpha^I \cdot \mathbf{p}^I + \beta^I m_q = \alpha^I \cdot \mathbf{p} + \beta^I m_q \quad (\text{A.18})$$

$$H_{II} = \alpha^{II} \cdot \mathbf{p}^{II} + \beta^{II} m_q = -\alpha^{II} \cdot \mathbf{p} + \beta^{II} m_q \quad (\text{A.19})$$

$$U_B(\mathbf{r}) = -\left(\frac{4}{3}\alpha_s\right)\frac{1}{r} \left[1 - \frac{\alpha^I \cdot \alpha^{II}}{2} + \frac{(\alpha^I \cdot \mathbf{r}_{12})(\alpha^{II} \cdot \mathbf{r}_{12})}{2r^3} \right] \quad (\text{A.20})$$

But a clever observation by [1] makes the above formula usable. The reasoning follows as, since we are interested in separating negative and positive energy solutions, we might as well do the separation in the beginning using the projection operators

$$\Lambda_{\pm}^I \equiv \frac{E_I \pm H_I}{2E_I} \quad \Lambda_{\pm}^{II} \equiv \frac{E_{II} \pm H_{II}}{2E_{II}} \quad (\text{A.21})$$

where

$$E_I \equiv \sqrt{m_I^2 + p^2} \quad E_{II} \equiv \sqrt{m_{II}^2 + p^2} \quad (\text{A.22})$$

In [11] this observation is made rigorous by considering, instead of our starting Hamiltonian, the Hermitian part of the three-dimensional Bethe-Salpeter equation written in coordinate space given as,

$$H\Psi(\mathbf{r}) = \left(H_I + H_{II} + \frac{1}{2} \left[\left\{ \Lambda_+^I \Lambda_+^{II} - \Lambda_-^I \Lambda_-^{II} \right\}, H_B(\mathbf{r}) \right]_+ \right) \Psi(\mathbf{r}) = E\Psi(\mathbf{r}) \quad (\text{A.23})$$

We now evaluate the anti-commutator of $U_B(\mathbf{r})$ with the projection operators. Noting that

$$\Lambda_+^I \Lambda_+^{II} - \Lambda_-^I \Lambda_-^{II} = \frac{(E_I + H_I)(E_{II} + H_{II})}{E_I E_{II}} - \frac{(E_I - H_I)(E_{II} - H_{II})}{E_I E_{II}} \quad (\text{A.24})$$

$$= \frac{E_{II} H_I}{E_I E_{II}} + \frac{E_I H_{II}}{E_I E_{II}} \quad (\text{A.25})$$

$$= \frac{H_I}{E_I} + \frac{H_{II}}{E_{II}} \quad (\text{A.26})$$

therefore,

$$\frac{1}{2} \left[\left\{ \Lambda_+^I \Lambda_+^{II} - \Lambda_-^I \Lambda_-^{II} \right\}, H_B(\mathbf{r}) \right]_+ = \frac{1}{2} \left[\frac{H_I}{E_I} + \frac{H_{II}}{E_{II}}, H_I \right]_+ \quad (\text{A.27})$$

$$+ \frac{1}{2} \left[\frac{H_I}{E_I} + \frac{H_{II}}{E_{II}}, H_I \right]_+ \quad (\text{A.28})$$

$$+ \frac{1}{2} \left[\frac{H_I}{E_I} + \frac{H_{II}}{E_{II}}, U_B \right]_+ \quad (\text{A.29})$$

Now observe that, for example,

$$\left[\frac{H_I}{E_I}, H_I(\mathbf{r}) \right]_+ = \left[\frac{H_I}{\sqrt{m_I^2 + p^2}}, H_I(\mathbf{r}) \right]_+ \quad (\text{A.30})$$

$$= \frac{1}{m_I} \left[H_I \left(\frac{p}{m} \right) - \frac{1}{2} \left(\frac{p}{m} \right)^2 + \dots, H_I(\mathbf{r}) \right]_+ \quad (\text{A.31})$$

where we have expanded in the powers of $\frac{p}{m}$. But we are only interested in the terms up to order $(\frac{1}{m})^2$, therefore discarding the higher order we arrive at.

$$\left[\frac{H_I}{E_I}, H_I(\mathbf{r}) \right]_+ \approx \frac{1}{m^2} [H_I p, H_I(\mathbf{r})]_+ \quad (\text{A.32})$$

Carrying out a similar analysis in all terms, we compute the commutation of H_B and positive and negative energy projectors, up to order $1/m^2$, which is given as,

$$H_I + H_{II} + \frac{1}{2} \left[\left\{ \Lambda_+^I \Lambda_+^{II} - \Lambda_-^I \Lambda_-^{II} \right\}, H_B(\mathbf{r}) \right]_+ = \mathcal{E}\mathcal{E} + \mathcal{O}\mathcal{E} + \mathcal{O}\mathcal{O} \quad (\text{A.33})$$

where,

$$\mathcal{E}\mathcal{E} = \frac{\epsilon}{2r} (\beta^I + \beta^{II}) - \frac{\epsilon}{8m^2} (\beta^I + \beta^{II}) \left[p^2, \frac{1}{r} \right]_+ \quad (\text{A.34})$$

$$\begin{aligned} \mathcal{O}\mathcal{E} &= \alpha^I \cdot \mathbf{p} + \frac{3\epsilon}{8m} \left[\alpha^I \cdot \mathbf{p}, \frac{1}{r} \right]_+ + \frac{i\epsilon}{8m} \alpha^I \times \sigma^{II} \cdot \left[\mathbf{p}, \frac{1}{r} \right] \\ &+ \frac{\epsilon}{8m} \left[\mathbf{p}, \frac{\mathbf{r}(\alpha^I \cdot \mathbf{r})}{r^3} \right]_+ \end{aligned} \quad (\text{A.35})$$

$$+ \frac{i\epsilon}{8m} \sigma^{II} \cdot \left[\mathbf{p} \times, \frac{\mathbf{r}(\alpha^I \cdot \mathbf{r})}{r^3} \right]_+ \quad (\text{A.36})$$

$$\begin{aligned} \mathcal{E}\mathcal{O} &= -\alpha_{II} \cdot \mathbf{p} - \epsilon \frac{3\epsilon}{8m} \left[\alpha^{II} \cdot \mathbf{p}, \frac{1}{r} \right]_+ - \frac{i\epsilon}{8m} \alpha^I \times \sigma^{II} \cdot \left[\mathbf{p}, \frac{1}{r} \right] \\ &- \frac{\epsilon}{8m} \left[\mathbf{p}, \frac{\mathbf{r}(\alpha^I \cdot \mathbf{r})}{r^3} \right]_+ \end{aligned} \quad (\text{A.37})$$

$$- \frac{i\epsilon}{8m} \sigma^{II} \cdot \left[\mathbf{p} \times, \frac{\mathbf{r}(\alpha^I \cdot \mathbf{r})}{r^3} \right]_+ \quad (\text{A.38})$$

Now Substituting above terms in Eqn[A.16] gives the desired Breit-Fermi interaction terms.

$$H_{BF} = -\frac{4\alpha_s}{3r} \quad (\text{A.39})$$

$$2m + \frac{\mathbf{p}^2}{m} - \frac{\mathbf{p}^4}{4m^3} \quad (\text{A.40})$$

$$-\frac{2\alpha_s}{3m_q^2} \left(\frac{\mathbf{p}^2}{r} + \frac{\mathbf{r}(\mathbf{r} \cdot \mathbf{p}) \cdot \mathbf{p}}{r^3} \right) \quad (\text{A.41})$$

$$+\frac{4\alpha_s}{3m_q^2} \delta(\mathbf{r}) \left(1 + \frac{8\pi}{3} \mathbf{S}_1 \cdot \mathbf{S}_2 \right) \quad (\text{A.42})$$

$$+2\frac{\alpha_s}{m_q^2 r^3} ((\mathbf{S}_1 + \mathbf{S}_2) \cdot \mathbf{L}) \quad (\text{A.43})$$

$$+\frac{4\alpha_s}{3m_q^2 r^3} \left(3 \frac{(\mathbf{S}_1 \cdot \mathbf{r})(\mathbf{S}_2 \cdot \mathbf{r})}{r^2} - \mathbf{S}_1 \cdot \mathbf{S}_2 \right) \quad (\text{A.44})$$

APPENDIX B

TENSOR INTERACTION COEFFICIENTS

In this part given the tensor interaction

$$V_{Tensor} = \frac{4}{3} \frac{\alpha_s}{m_q^2 r^3} \left(3 \frac{(\mathbf{S}_1 \cdot \mathbf{r})(\mathbf{S}_2 \cdot \mathbf{r})}{r^2} - \mathbf{S}_1 \cdot \mathbf{S}_2 \right) \quad (\text{B.1})$$

we are interested in evaluating matrix elements of the tensor interaction coefficients,

$$\left\langle 3 \frac{(\mathbf{S}_1 \cdot \mathbf{r})(\mathbf{S}_2 \cdot \mathbf{r})}{r^2} - \mathbf{S}_1 \cdot \mathbf{S}_2 \right\rangle = \langle T_{12} \rangle \quad (\text{B.2})$$

Noting that,

$$(\mathbf{S} \cdot \mathbf{r})^2 = (\mathbf{S}_1 \cdot \mathbf{r})^2 + (\mathbf{S}_2 \cdot \mathbf{r})^2 + 2(\mathbf{S}_2 \cdot \mathbf{r})(\mathbf{S}_1 \cdot \mathbf{r}) \quad (\text{B.3})$$

$$= \frac{1}{4}(\sigma_1 \cdot \mathbf{r})^2 + \frac{1}{4}(\sigma_2 \cdot \mathbf{r})^2 + 2(\mathbf{S}_2 \cdot \mathbf{r})(\mathbf{S}_1 \cdot \mathbf{r}) \quad (\text{B.4})$$

$$= \frac{1}{2}\mathbf{r}^2 + 2(\mathbf{S}_2 \cdot \mathbf{r})(\mathbf{S}_1 \cdot \mathbf{r}) \quad (\text{B.5})$$

and

$$\mathbf{S}_1 \cdot \mathbf{S}_2 = \frac{1}{2}(\mathbf{S}^2 - \mathbf{S}_1^2 - \mathbf{S}_2^2) \quad (\text{B.6})$$

$$= \frac{1}{2}\left(\mathbf{S}^2 - \frac{3}{2}\right) \quad (\text{B.7})$$

We obtain the coefficient in terms of the total spin operator.

$$\frac{1}{2} \left(3 \frac{(\mathbf{S} \cdot \mathbf{r})^2}{r^2} - \mathbf{S}^2 \right) \quad (\text{B.8})$$

In spherical coordinates the total spin matrix is given as,

$$\mathbf{S} = S_x \hat{x} + S_y \hat{y} + S_z \hat{z} \quad \mathbf{r} = r(\sin \theta \cos \phi \hat{x} + \sin \theta \sin \phi \hat{y} + \cos \theta \hat{z}) \quad (\text{B.9})$$

Therefore the scalar product is,

$$\frac{(\mathbf{S} \cdot \mathbf{r})^2}{r^2} = S_x^2 \sin^2 \theta \cos^2 \phi + S_y^2 \sin^2 \theta \sin^2 \phi + S_z^2 \cos^2 \theta \quad (\text{B.10})$$

$$+(S_x S_y + S_y S_x) \sin^2 \theta \cos \phi \sin \phi \quad (\text{B.11})$$

$$+(S_x S_z + S_z S_x) \sin \theta \cos \theta \cos \phi \quad (\text{B.12})$$

$$+(S_y S_z + S_z S_y) \sin \theta \cos \theta \sin \phi \quad (\text{B.13})$$

We are interested in finding the matrix elements in the $\langle j, l, s, m_j |$ basis, which can be expressed as,

$$\Sigma \langle j, \widetilde{l, s, m_j} | l', m'_l, s', m'_s \rangle \left\{ \langle l', m'_l, s', m'_s | T_{12} | l'', m''_l, s'', m''_s \rangle \right\} \langle l'', m''_l, s'', m''_s | j, l, s, m_j \rangle \quad (\text{B.14})$$

where the summation is over primed and double primed states. Evaluating the matrix elements in the curly brackets and expressing the various combinations of sine and cosine terms in terms spherical harmonics, we find,

$$\langle l', m'_l, s', m'_s | T_{12} | l'', m''_l, s'', m''_s \rangle = \quad (\text{B.15})$$

$$c_{++} \left(\frac{2\pi}{3} \right) \langle l', m'_l, s', m'_s | Y_1^{-1} | l'', m''_l, s'', m''_s + 2 \rangle \quad (\text{B.16})$$

$$+ c_{--} \left(\frac{2\pi}{3} \right) \langle l', m'_l, s', m'_s | Y_1^1 | l'', m''_l, s'', m''_s - 2 \rangle \quad (\text{B.17})$$

$$+ \left(\frac{2\pi}{3} \right) \langle l', m'_l, s', m'_s | (-c_0 Y_1^{-1} Y_1^1 + 2m''_s (Y_1^0)^2) | l'', m''_l, s'', m''_s \rangle \quad (\text{B.18})$$

$$+ c_+ \frac{2\sqrt{2}\pi}{3} (2m''_s + 1) \langle l', m'_l, s', m'_s | Y_1^{-1} Y_1^0 | l'', m''_l, s'', m''_s + 1 \rangle \quad (\text{B.19})$$

$$+ c_- \frac{2\sqrt{2}\pi}{3} (2m''_s - 1) \langle l', m'_l, s', m'_s | Y_1^1 Y_1^0 | l'', m''_l, s'', m''_s - 1 \rangle \quad (\text{B.20})$$

where coefficients arising from the action of raising and lowering operators are,

$$c_{++} = \sqrt{(j'' - m'')(j'' + m'' + 1)} \sqrt{(j'' - m'' - 1)(j'' + m'' + 2)} \quad (\text{B.21})$$

$$c_{--} = \sqrt{(j'' + m'' - 1)(j'' - m'' + 2)} \sqrt{(j'' + m'')(j'' - m'' + 1)} \quad (\text{B.22})$$

$$c_+ = \sqrt{(j'' - m'')(j'' - m'' + 1)} \quad c_- = \sqrt{(j'' + m'')(j'' - m'' + 1)} \quad (\text{B.23})$$

$$c_0 = 2(j''(j'' + 1) - m'') \quad (\text{B.24})$$

To evaluate the spherical harmonics together with the inner product of $|lm_l\rangle$ states we use the $3jm$ symbols to evaluate the integral between the products of three spherical harmonics

$$\int Y_{l_1}^{m_1} Y_{l_2}^{m_2} Y_{l_3}^{m_3} \sin \theta d\theta d\phi = N_2(l_1, l_2, l_3) \begin{pmatrix} l_1 & l_2 & l_3 \\ 0 & 0 & 0 \end{pmatrix} \begin{pmatrix} l_1 & l_2 & l_3 \\ m_1 & m_2 & m_3 \end{pmatrix} \quad (\text{B.25})$$

where,

$$\begin{pmatrix} l_1 & l_2 & l_3 \\ m_1 & m_2 & m_3 \end{pmatrix} = \frac{(-1)^{j_1 - j_2 - m_3}}{\sqrt{2j_3 + 1}} \langle j_1 m_1 j_2 m_2 | j_3 - m_3 \rangle \quad (\text{B.26})$$

and

$$N_3(l_1, l_2, l_3) = \sqrt{\frac{(2l_1 + 1)(2l_2 + 1)(2l_3 + 1)}{4\pi}} \quad (\text{B.27})$$

Therefore for example the first term gives

$$c_{++} \left(\frac{2\pi}{3} \right) \langle l', m'_l, s', m'_s | Y_1^{-1} | l'', m''_l, s'', m''_s + 2 \rangle \quad (\text{B.28})$$

$$= c_{++} \left(\frac{2\pi}{3} \right) \langle l', m'_l | Y_1^{-1} | l'', m''_l \rangle \delta_{s', s''} \delta_{m'_s, m''_s + 2} \quad (\text{B.29})$$

$$= c_{++} \left(\frac{2\pi}{3} \right) \left\{ \int Y_{l'}^{*m'_l} Y_1^{-1} Y_{l''}^{m''_l} \sin \theta d\theta d\phi \right\} \delta_{s', s''} \delta_{m'_s, m''_s + 2} \quad (\text{B.30})$$

$$= c_{++} \left(\frac{2\pi}{3} \right) N_2(l_1, l_2, l_3) \begin{pmatrix} l' & 1 & l'' \\ 0 & 0 & 0 \end{pmatrix} \begin{pmatrix} l' & 1 & l'' \\ -m'_l & -1 & m''_l \end{pmatrix} \delta_{s', s''} \delta_{m'_s, m''_s + 2} \quad (\text{B.31})$$

Next the remaining Clebsch Gordon coefficients are expressed in terms of $3jm$ symbols, using Eqn[B.26], which we will show only for the first term,

$$= \sum_{l'', j} \begin{pmatrix} l' & 1 & \tilde{j} \\ m'_l & 1 & -\tilde{m}_{\tilde{j}} \end{pmatrix} \begin{pmatrix} l' & 1 & l'' \\ 0 & 0 & 0 \end{pmatrix} \begin{pmatrix} l' & 1 & l'' \\ -m'_l & -1 & m''_l \end{pmatrix} \begin{pmatrix} l' & 1 & j \\ m''_l & -1 & m_j \end{pmatrix} \quad (\text{B.32})$$

Where we have used the orthogonality relation to deduce, $m''_j = -m'_j = -1$. Using the selection rules we obtain $\tilde{m}_{\tilde{j}} = 1 - m_j$, and using the orthogonality relations by carrying out the summations, and carrying out a similar analysis in all terms one finds that the tensor operator has non-vanishing diagonal matrix elements only between $L > 0$ spin-triplet states

and its value is given by

$$T_{Tensor} = 3 \frac{(\vec{S}_i \cdot r)(\vec{S}_j \cdot r)}{r^2} - \vec{S}_i \cdot \vec{S}_j = \begin{cases} -\frac{l}{2(2l+3)} & J = L + 1 \\ 1/2 & J = L \\ -\frac{(l+1)}{3(2l-1)} & J = L - 1 \\ 0 & L = 0 \text{ or } S = 0 \end{cases} \quad (\text{B.33})$$